iScience

CellPress
OPEN ACCESS

Article

Hippo-PKCζ-NFκB signaling axis: A druggable modulator of chondrocyte responses to mechanical stress

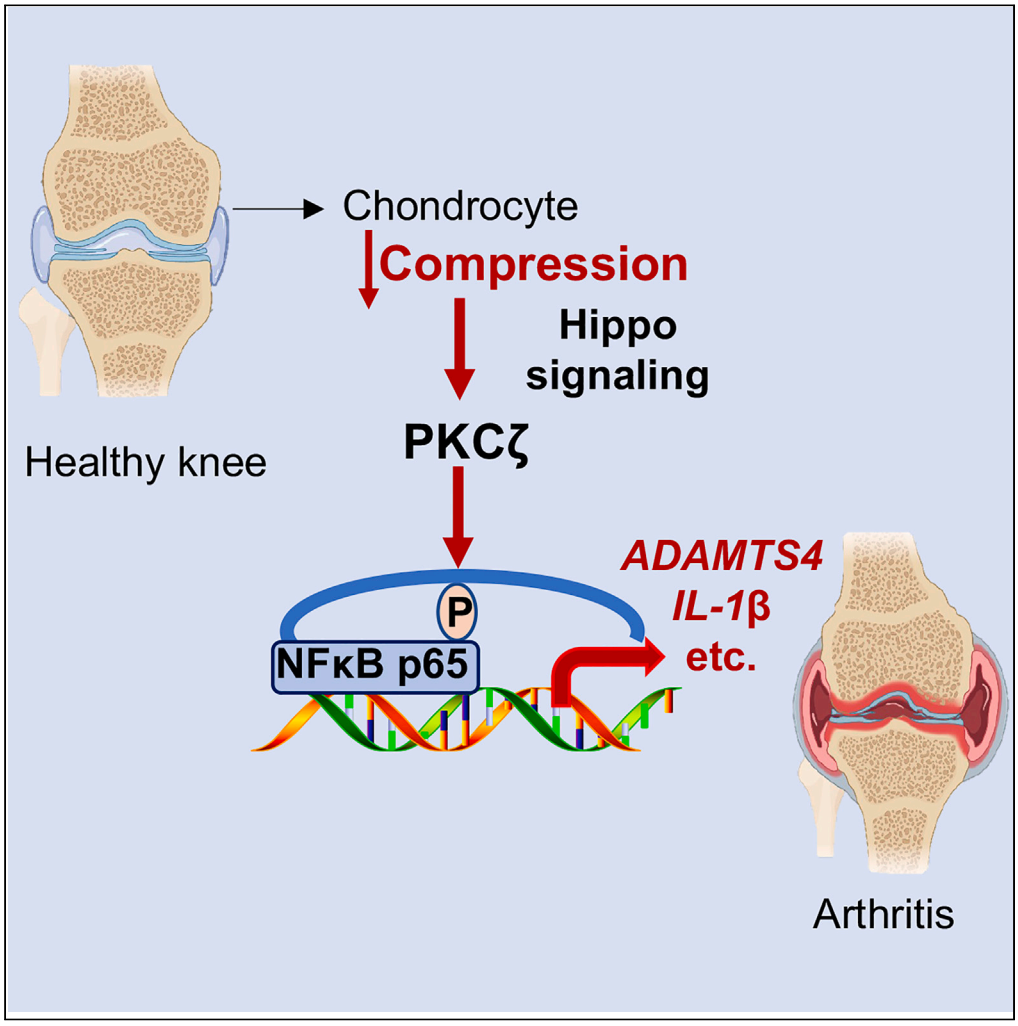

Xiaomin Cai, Christopher Warburton, Olivia F. Perez, ..., Thomas M. Best, Chun-Yuh Huang, Zhipeng Meng

c.huang1@miami.edu (C.-Y.H.)
zxm282@med.miami.edu (Z.M.)

Highlights

Elucidating the roles and interplay of Hippo signaling and PKC during mechanoinflammation

The first study to investigate the effects of mechanical compression on Hippo signaling

Unveiling the therapeutic potential of targeting Hippo signaling or PKCζ in osteoarthritis

Cai et al., iScience 27, 109983
June 21, 2024
https://doi.org/10.1016/j.isci.2024.109983

iScience

CellPress
OPEN ACCESS

Article

Hippo-PKCζ-NFκB signaling axis: A druggable modulator of chondrocyte responses to mechanical stress

Xiaomin Cai,[1,2] Christopher Warburton,[3,7] Olivia F. Perez,[3,7] Ying Wang,[1,2,7] Lucy Ho,[4] Christina Finelli,[4] Quinn T. Ehlen,[3] Chenzhou Wu,[1,2] Carlos D. Rodriguez,[1,2] Lee Kaplan,[4,5,6] Thomas M. Best,[4,5,6] Chun-Yuh Huang,[2,3,4,6,*] and Zhipeng Meng[1,2,3,8,*]

SUMMARY

Recent studies have implicated a crucial role of Hippo signaling in cell fate determination by biomechanical signals. Here we show that mechanical loading triggers the activation of a Hippo-PKCζ-NFκB pathway in chondrocytes, resulting in the expression of NFκB target genes associated with inflammation and matrix degradation. Mechanistically, mechanical loading activates an atypical PKC, PKCζ, which phosphorylates NFκB p65 at Serine 536, stimulating its transcriptional activation. This mechanosensitive activation of PKCζ and NFκB p65 is impeded in cells with gene deletion or chemical inhibition of Hippo core kinases LATS1/2, signifying an essential role of Hippo signaling in this mechanotransduction. A PKC inhibitor AEB-071 or PKCζ knockdown prevents p65 Serine 536 phosphorylation. Our study uncovers that the interplay of the Hippo signaling, PKCζ, and NFκB in response to mechanical loading serves as a therapeutic target for knee osteoarthritis and other conditions resulting from mechanical overloading or Hippo signaling deficiencies.

INTRODUCTION

Knee osteoarthritis (KOA) is a prevalent degenerative joint condition affecting about 30% of individuals over the age of 60 in the United States.[1] The exact pathophysiology of osteoarthritis (OA) is multifaceted and not yet fully understood. Risk factors, including obesity, aging, joint trauma, and female gender, are correlated with the development and progression of KOA. Obesity is considered one of the greatest modifiable risk factors for OA.[2] The increased mechanical loading on weight-bearing joints due to obesity contributes to KOA development and progression. Post-traumatic OA is another concern where a known precipitating insult to the joint from an external mechanical force causes injuries to the articular cartilage and/or other tissues (e.g., ligament and subchondral bone), leading to OA.[3–5] However, the mechanisms by which mechanical loading triggers OA pathogenesis remain to be defined for the development of preventative therapeutic strategies.[2,5]

The development of OA is a complex process involving metabolic disorders and systemic and local inflammation resulting from obesity.[1,2,6] These factors interplay with repetitive mechanical stress or acute mechanical injury to the joints, leading to joint destruction and exacerbating pain and disability. Mechanotransduction signaling pathways of chondrocytes sense increased mechanical stress and subsequently trigger the production of cytokines and metalloproteinases, leading to the degradation of surface articular cartilage.[7–10] The major role of articular cartilage within the joint is to provide a smooth, lubricated surface for articulation as well as to facilitate the transmission of applied forces with minimal frictional loads.[11] Notably, articular cartilage is avascular and devoid of lymph tissue, which limits its ability to adequately repair subsequent injury.[3,12] The knee joint experiences numerous compressive loading cycles throughout the day. Compressive forces can be static, such as when standing, or dynamic, such as with acting movement, or jumping. Chondrocytes within the cartilage sense and respond to the compressive loads by regulating and secreting essential cartilaginous extracellular matrix (ECM) components, including collagens and proteoglycans.[13] However, an overload of mechanical stress on chondrocytes leads to inflammatory conditions, resulting in cartilage destruction and chondrocyte apoptosis.[14]

[1]Department of Molecular and Cellular Pharmacology, Miller School of Medicine, Miami, FL, USA
[2]Sylvester Comprehensive Cancer Center, University of Miami Miller School of Medicine, Miami, FL, USA
[3]USOAR Scholar Program, Medical Education, University of Miami Miller School of Medicine, Miami, FL, USA
[4]Department of Biomedical Engineering, University of Miami, Coral Gables, FL, USA
[5]Department of Orthopedics, University of Miami, Miami, FL, USA
[6]UHealth Sports Medicine Institute, University of Miami, Miami, FL, USA
[7]These authors contributed equally
[8]Lead contact
*Correspondence: c.huang1@miami.edu (C.-Y.H.), zxm282@med.miami.edu (Z.M.)
https://doi.org/10.1016/j.isci.2024.109983

Understanding the mechanisms of mechanotransduction is crucial for developing new therapies that prevent cartilage destruction and chondrocyte apoptosis. The Hippo pathway, first discovered in *Drosophila*, has been recognized as a conserved signaling pathway in regulating organ development, regeneration, and carcinogenesis via integrating biochemical and mechanical cues that reshape cellular transcription programs.[15–18] The core of the mammalian Hippo pathway is a kinase cascade of the mammalian sterile twenty kinases ½ (MST1/2) and the large tumor suppressor kinase ½ (LATS1/2). Biochemical and biomechanical signals can act through this kinase cascade to phosphorylate and inactivate yes-associated protein (YAP) and transcriptional coactivator with PDZ-binding motif (TAZ), two transcription co-factors that initiate the expression of genes for cell cycling, mobility, and stemness. While the Hippo pathway effector YAP has been implicated in the development of OA, its precise pathogenic roles appear to be context dependent and require further investigation.[19,20]

The Hippo signaling is widely recognized as the best-characterized pathway for mechanosensing and mechanotransduction.[10,21–23] Given that OA can be induced by mechanical overload, it is essential to understand the exact functional roles of the Hippo signaling in the development of OA. Therefore, our study utilized a model of mechanical loading on 3D-cultured chondrocytes to investigate the regulation and functional significance of LATS1/2 and YAP/TAZ in the response of chondrocytes to overload. We discovered that proper Hippo signaling is required for mechanical loading to induce inflammation and matrix degradation through a protein kinase C (PKC)/nuclear factor-kappaB (NFκB) signaling axis. We further showed that the functional interplay between PKC and Hippo signaling is required for NFκB-activated inflammation and matrix degradation and thus serves as a new target for OA therapeutic intervention.

RESULTS

Mechanical overload alters the expression of KOA-associated genes

It is believed that mechanical loading leads to KOA by triggering inflammation and other immune responses of chondrocytes. We analyzed an RNAseq dataset comparing preserved and damaged cartilages, which represent early and late human KOA, respectively.[24] We observed that there were upregulated immune responses in the early stage of KOA development compared with the late stage in gene set enrichment analysis (GSEA) (Figure 1A). Similarly, the expression of collagen-related extracellular matrix genes also underwent significant changes during KOA development (Figure S1A).

We established both 2- (2D) and 3-dimensional (3D) *in vitro* models to study the gene transcriptional responses of chondrocytes to mechanical overload (Figures 1B and 1C). We focused on the mRNA levels of two key OA genes, interleukin-1 beta (*IL1β*) and A disintegrin and metalloproteinase with thrombospondin motifs 4 (*ADAMTS4*), associated with inflammatory responses and extracellular matrix degradation, respectively. *IL1β* is a cytokine that induces articular cartilage inflammation and is elevated in OA. *ADAMTS4* is an aggrecanase that cleaves aggrecan, the major proteoglycan found in articular cartilage, which can lead to loss of cartilage function and destruction in OA.[25,26]

For the compression study with 2D culture, we followed a well-established protocol.[27,28] We seeded C28/I2 human chondrocytes onto trans-well membranes with 0.4 μm pore and covered the chondrocytes with agarose discs as water-permeable buffering. When the cell density reached 80%, an 8.9g stainless-steel cylinder was placed on top of the agarose disk for 16 h (Figure 1B). This level of mechanical compression has been shown to significantly impact cell-matrix interaction and cell mobility. However, it cannot significantly increase the expression of *IL1β* and even reduce the expression of *ADAMTS4* in these 2D cultured chondrocytes (Figure 1D).

For the 3D culture system, we embedded chondrocytes into agarose discs and applied compression to the agarose discs using a compression bioreactor (Figures 1C and S1B) to induce deformation that mimics mechanical overload caused by overweight or mechanical impact to joints as described previously.[13,29] Twenty percent strain was applied to chondrocytes for 4 h to evaluate the association between strain magnitude and cell mechanoresponses. With this model, we consistently observed that mechanical loading significantly induces the expression of *IL1β* and *ADAMTS4* (Figure 1E) as well as OA-associated genes, such as *ADAMTS5* and *MMP9* (Figure S2). This suggested the suitability of this 3D model system for studying the pathogenesis process. Therefore, the 3D model was thereafter used in this study to define the mechanisms by which mechanical overload activates transcriptional programs for inflammation and matrix degradation.

Mechanical overload activates NFκB and Hippo signaling

NFκB plays a crucial role in OA-associated processes, including synovial inflammation and chondrocyte catabolism.[1,2,30] The NFκB family of transcription factors activates the expression of inflammatory cytokines (i.e., *IL1β*) and matrix-degrading enzymes (i.e., *ADAMTS4*).[31,32] It is speculated that NFκB can be directly activated by mechanical loading.[33,34] This notion is consistent with our RT-qPCR results of *IL1β* and *ADAMTS4* gene expression (Figure 1E).

We, therefore, tested whether NFκB can be activated by mechanical compression in our 3D model. Mechanical loading strongly increased Serine 536 (S536) phosphorylation of the classical NFκB member p65 but did not affect Serine 529 phosphorylation (Figure 2A). S536 phosphorylation of p65 is well known to promote the transcriptional activity of p65 independent of IκB, the endogenous negative regulator of p65.[35–37] However, we did not observe increased phosphorylation of IκB or increased proteolysis of p105, indicating that mechanical overload may act through a non-classical NFκB mechanism to phosphorylate p65 at S536 and thus activate p65.[37]

We also examined whether mechanical compression results in any form of cell death. We therefore first profiled chondrocytes for their apoptosis but we did not observe increased cleavage of PARP, caspase 3, or caspase 8, which are landmark events of apoptosis[38] (Figure 2B). In addition, we did not observe increased levels of autophagy and necroptosis by checking cleavage of LC3B and phosphorylation of RIP and MLKL (Figure 2C).[39,40] These results also helped us rule out the possibility that the NFκB activation induced by mechanical loading is

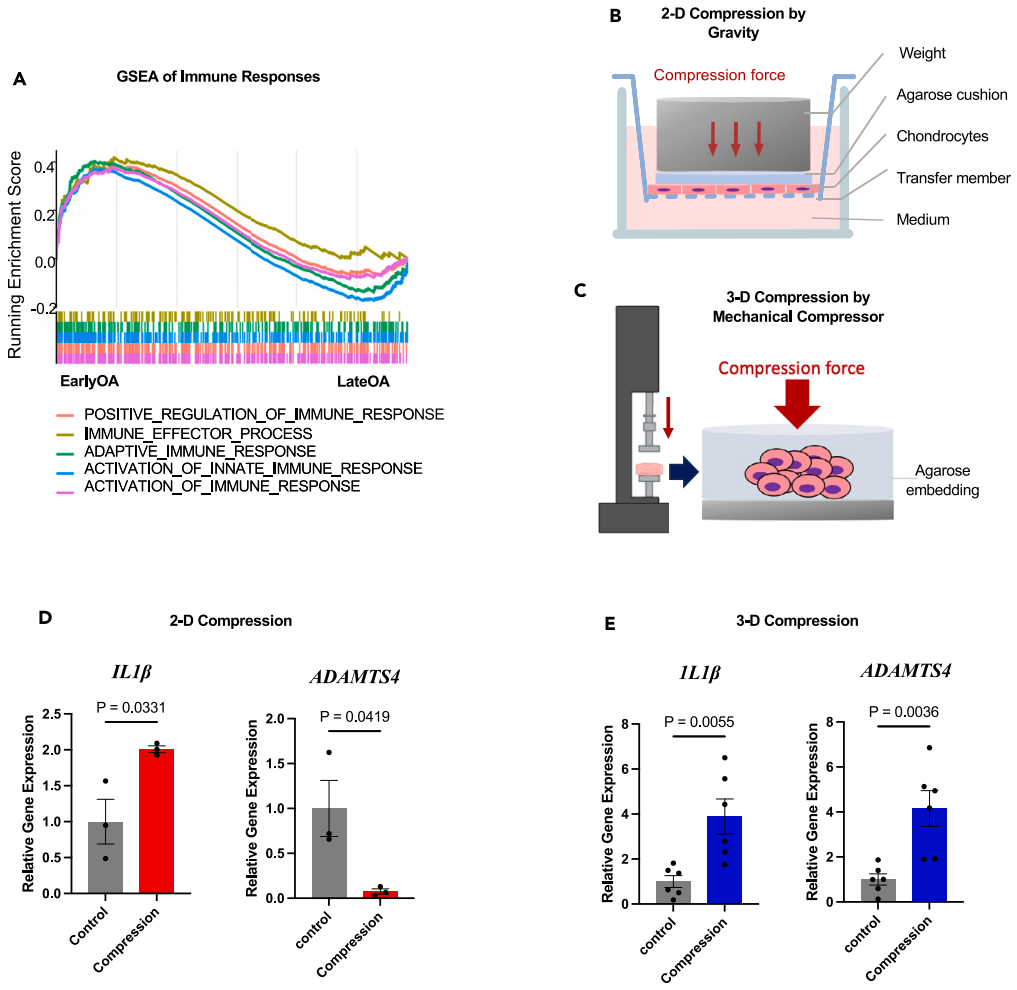

Figure 1. Differential responses of chondrocytes to mechanical compression in 2-dimensional (2D) and 3-dimensional (3D) models

(A) GSEA analyses of differentially regulated genes identified in RNAseq of patients in early and late osteoarthritis (OA) development.

(B) A diagram of 2D model of chondrocyte compression generated by gravity/weight.

(C) A diagram of 3D model of chondrocyte compression generated by a mechanical compressor.

(D) RT-qPCR analyses of *IL1β* and *ADAMTS4* gene expression in the 2D compression model. Student t tests were used to determine the difference between the control and the compressed chondrocytes; $n = 3$. Error bars represent the standard error of the mean (SEM). Data are presented as mean ± SEM.

(E) *IL1β* and *ADAMTS4* gene expression of chondrocytes in the 3 D compression model. Student t tests were used to determine the difference between the control and the compressed chondrocytes; $n = 6$.

secondary to apoptosis, autophagy, or necroptosis caused by compression and cell deformation. There have been reports indicating mTORC1 signaling can also respond to mechanical load in some scenarios and thus contribute to OA development.[41,42] However, we did not observe an increased mTORC1 activity, shown by the Threonine 389 (T389) phosphorylation of mTORC1 substrate S6K, which is the most sensitive and specific readout for mTORC1 activity (Figure 2D). We did not observe consistent phosphorylation at Serine 235/236 (S235/246) of S6, which are substrate sites for S6K.

As YAP, the Hippo pathway effector is the best-characterized mechanotransduction transcription factor and is also implicated in NFκB regulation during OA, though whether this potential role of the Hippo-YAP signaling involves in mechanical loading was still unclear.[19,20] We first analyzed the Hippo signature genes in GSEA with the RNAseq dataset comparing preserved and damaged cartilages and discovered a potential alteration of Hippo signaling in OA development[24] (Figure 2E). However, as Hippo pathway components are mostly regulated at post-translation levels, we therefore investigated the YAP regulation by mechanical loading with immunoblots. The activity of YAP is mainly determined by its phosphorylation status, as hyperphosphorylated YAP cannot enter the nucleus to initiate gene expression.[10,21–23] Therefore, we performed a Phostag electrophoresis where an upshift of target protein bands indicates its hyperphosphorylation. We found that mechanical loading strongly induced YAP phosphorylation (Figure 2F). Consistently, the mechanical loading decreased the level of YAP that was not phosphorylated by LATS1/2 (non-phosphorylated YAP) and the total protein level of TAZ, which is negatively correlated with its phosphorylation status.

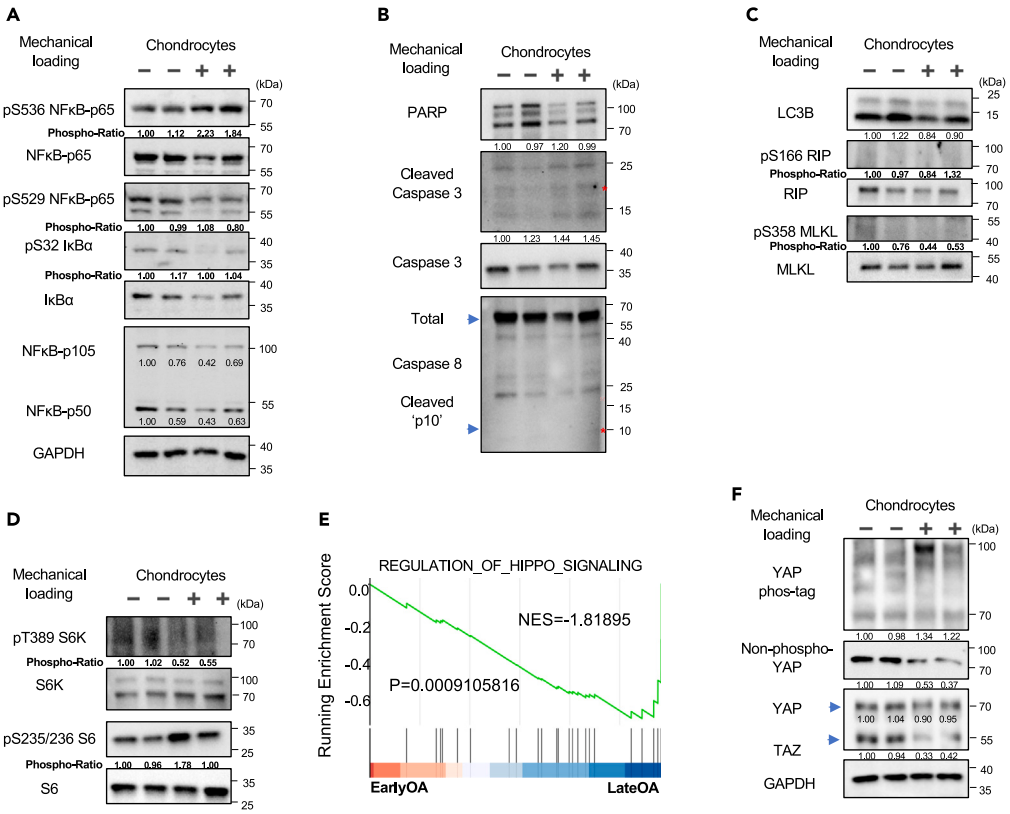

Figure 2. Mechanical compression activates NFκB and Hippo signaling in chondrocytes

(A) Mechanical compression induces phosphorylation of NFκB p65 at Serine 536. The quantification of phospho-proteins was normalized to the corresponding total proteins. The compression is to deform cells by 20% in volume and the duration is 4 h. Biological duplicates were tested.

(B and C) The mechanical compression applied to chondrocytes does not lead to cell death in the acute phase (within 4 h). Markers for programmed cell death (B), autophagy, and necroptosis (C) were determined by western blot. *, indicates predicted bands for the cleaved caspases.

(D) The effects of mechanical compression on mTORC1 downstream substrate p70-S6K.

(E) GSEA analysis of Hippo signature genes in early and late OA of human patients. NES, normalized enrichment score.

(F) Mechanical compression controls YAP phosphorylation. For YAP phostag analysis, phosphorylated YAP migrates more slowly on this gel. Therefore, the bottom band indicates hypophosphorylated YAP while the upper band indicates hyperphosphorylated YAP.

The biomechanical microenvironment regulates the transcriptional activity of YAP

Compared to 2D monolayers, 3D agarose culture models may better maintain the chondrocyte phenotype and better mimic the physiological microenvironment under compression.[43] *In vitro* culture may lead to de-differentiation of chondrocytes, which can be measured by the loss of characteristic phenotypic markers of chondrocytes, such as collagen type II (COL2A1), aggrecan (ACAN), and SRY-box transcription factor 9 (SOX9).[44,45] We found that the expression of *ACAN* and *SOX9* in chondrocytes is similar between 2D and 3D cultures (Figure 3A). However, the expression of *COL2A1* is much higher in 3D than in 2D culture, indicating that 3D culture may better preserve the differentiation status of chondrocytes.

A recent study suggested that the biomechanical microenvironment acts through YAP/TAZ to suppress chondrogenic gene expression.[46] We therefore next determined whether the biomechanical conditions (3D vs. 2D) regulate the Hippo pathway activity in chondrocytes. Our results showed significant differences in the expression of four classical YAP target genes (*CTGF*, *CYR61*, *ANKRD1*, and *AMOTL2*) between 2D and 3D cultures (Figure 3B). All genes in the 2D culture environment were higher when compared to the 3D cultures, which were grown in a softer matrix and in an anchorage-independent status that recapitulates the features of a normal knee microenvironment.[47] These results are consistent with the notion that cell attachment to a stiff matrix activates YAP by inactivating the Hippo pathway.[48] Therefore, we next determined the Hippo kinase activation status by examining the phosphorylation of LATS kinase at its phosphorylation motif (pLATS-HM), which is substantially higher in the 3D cultures than in 2D-cultured chondrocytes (Figure 3C). Consistently, phosphorylation of YAP, as shown by our phostag electrophoresis analyses, is also strongly increased at 3D compared with at 2D.

To further support the notion that the different stiffness levels may in part account for different YAP activities, we compared the expression of YAP target genes *CTGF* and *CYR61* in chondrocytes of the 2D, 3D cultures, and chondrocytes growing on fibronectin-coated

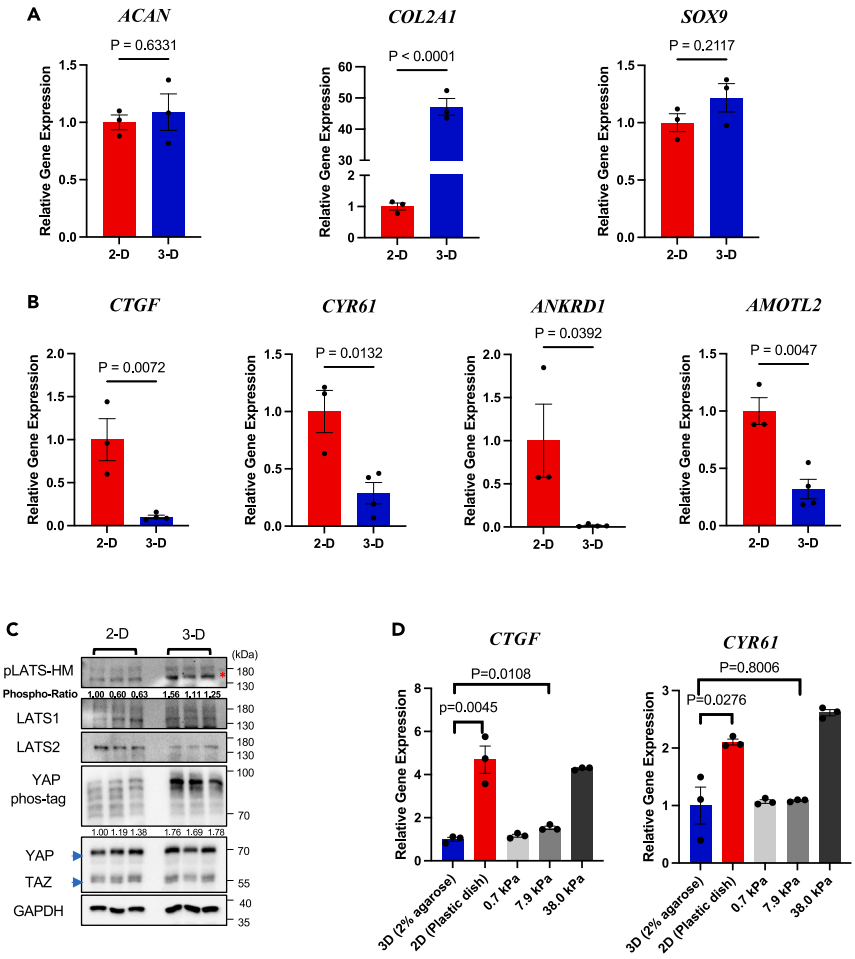

Figure 3. Differential activation status of the Hippo pathway in 2-dimensional (2D) and 3-dimensional (3D) culture

(A) The expression of chondrocyte marker genes was compared between 2D and 3D culture by RT-qPCR. The data are presented as mean ± SEM.

(B) Gene expression analysis of YAP target genes *CTGF*, *CYR61*, *ANKRD1*, and *AMOTL2* in chondrocytes under 2D or 3D culture conditions.

(C) Immunoblot for the phosphorylation of Hippo pathway core components LATS1/2 and YAP. * indicates specific bands for pLATS-HM.

(D) Comparing chondrocytes in 3D agarose gel with those in 2D plastic culture dish and comparing chondrocytes in 3D agarose gel with those on polyacrylamide hydrogels of 7.9 kPa for the expression of *CTGF* and *CYR61*. For all RT-qPCR analyses in Figure 3, student's t tests were used; $n = 3$.

polyacrylamide hydrogels with different stiffness levels.[16] It should be noted the 2% agarose gel for 3D culture is estimated to have a stiffness of about 8 kPa.[49] We indeed found that the expression of YAP target genes, *CTGF* and *CYR61*, is similar in chondrocytes embedded in 2% agarose 3D culture and on 8 kPa (or lower stiffness) polyacrylamide hydrogels (Figure 3D). However, cells growing on hydrogels with a stiffness >38 kPa and on plastic dishes show similarly high levels of *CTGF* and *CYR61*. This is consistent with very recent studies reporting that stiffness activates YAP and subsequently blunts inflammatory responses.[50–52]

Furthermore, we also determine the effect of the agarose concentration, which is positively correlated with the stiffness, on the expression of YAP target genes. A higher concentration of agarose (corresponding to higher stiffness) increases the expression of YAP target genes *CTGF*, *CYR61*, and *ANKRD1* (Figure S3A). Moreover, the basal phosphorylation of NFκB p65-S536, without mechanical compression to the chondrocytes, negatively correlates with the agarose concentration (Figure S3B). Consistently, the basal expression of *IL1β*, without mechanical compression, also negatively correlates with the agarose concentration (Figure S3C).

The physiological biomechanical microenvironment is essential for the proper regulation of Hippo signaling in chondrocytes

The activity of the Hippo pathway is normally high to maintain the quiescence of cells and prevent aberrant cell proliferation. To define the functional role of the Hippo pathway in the 2D and 3D chondrocyte cultures, we used CRISPR/Cas9 to delete LATS1/2 or YAP genes in chondrocytes (Figures 4A and 4B). Lentiviruses expressing Cas9 and sgRNAs for LATS1, LATS2, or YAP were used to infect chondrocytes to generate knockout cell pools for each gene. The LATS kinase activity is tightly regulated by cell confluence.[21,53] Our phostag electrophoresis data clearly showed that deletion of both LATS1 and LATS2 (sgLATS) strongly comprised YAP protein phosphorylation induced by cell

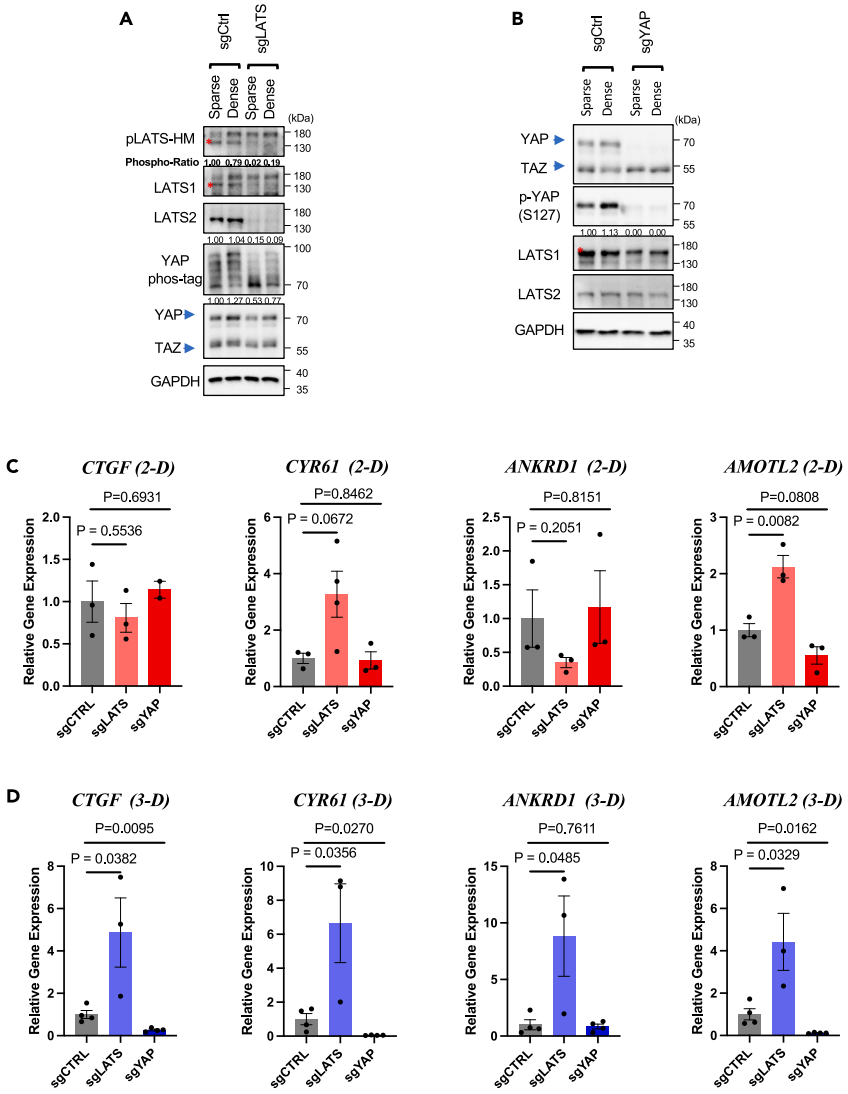

Figure 4. Deletion of LATS1/2 and YAP/TAZ by CRISPR/Cas9 in chondrocytes

(A) Immunoblot showing the expression and phosphorylation of LATS1/2 and YAP/TAZ in chondrocyte pool with the expression of Cas9 and sgRNAs targeting LATS1/2. The same number of cells were seeded onto 6-well (sparse) and 24-well (dense) plates. * indicates the specific bands for pLATS-HM.

(B) Expression or phosphorylation of YAP or TAZ after CRISPR/Cas9-mediated gene deletion in chondrocytes.

(C and D) RT-qPCR of YAP target genes at 2D or 3D. For all RT-qPCR analyses in Figure 4, student's t tests were used; $n = 3$. The data are presented as mean ± SEM.

confluence (Figure 4A), affirming the deficiency in the Hippo kinase cascade. Moreover, we achieved highly efficient gene knockout of YAP in the cells (Figure 4B).

Surprisingly, the deletion of LATS1/2 may decrease *CTGF* and *ANKRD1* mRNA levels in 2D culture but tends to increase the expression of *CYR61* and *AMOTL2* (Figure 4C). The absence of an increase in the YAP target gene expression is likely because the activity of LATS1/2 was already very low due to the stiffness of 2D cultured chondrocytes, which is known to inactivate LATS1/2 and thus activate YAP.[21,54] Deletion of LATS1/2 (in sgLATS1/2 cells) may not be able to increase already very high YAP activity and YAP target gene expression further. This notion is also consistent with the results of stiffness effects on the YAP target gene in this study (Figures 3D and S3).

On the other hand, deletion of YAP alone cannot reduce the expression of some YAP target genes (Figure 4C), which may be due to the compensatory activation or over-expression of TAZ in the YAP knockout cell pool (Figure 4B). Contrary to the 2D culture, the chondrocytes at the 3D culture maintain the Hippo pathway activity (Figure 4D). Deletion of LATS1/2 (sgLATS) can robustly increase the expression of YAP target genes (*CTGF*, *CYR61*, *ANKRD1*, and *AMOTL2*) in 3D cultured chondrocytes. It should be noted that, though the activity of YAP is much lower at 3D than that at 2D, chondrocytes still maintain a certain level of YAP activity at the 3D culture, as deletion of YAP further reduced the expression of the YAP target genes (*CTGF*, *CYR61*, and *AMOTL2*).

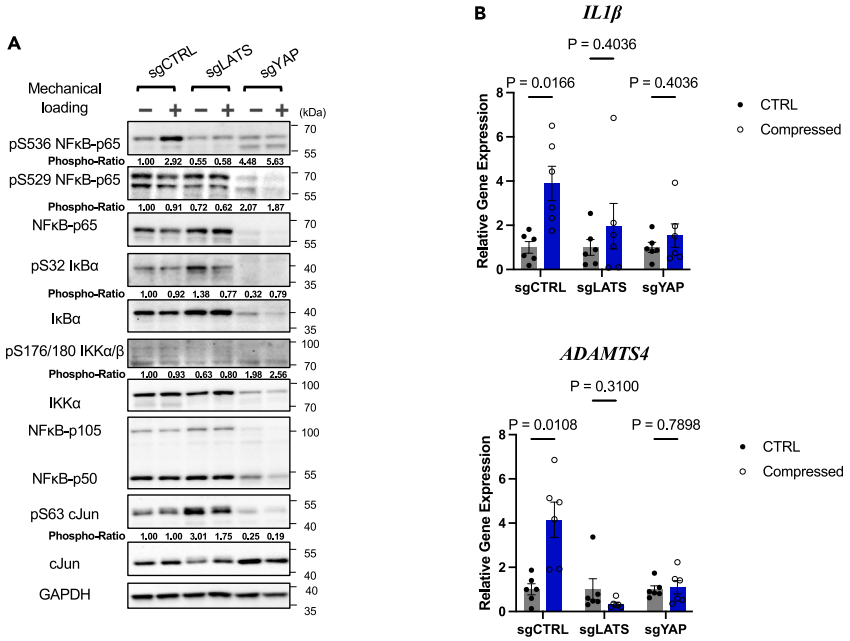

Figure 5. The Hippo pathway is required for mechanical loading-induced NFκB activation

(A) Deletion of either LATS or YAP abolishes NFκB p65 phosphorylation at Serine 536.

(B) The expression of NFκB target genes *IL1β* and *ADAMTS4* in the control, LATS1/2-KO (sgLATS1/2), and YAP-KO (sgYAP). Multiple t tests were used; $n = 6$. The data are presented as mean ± SEM.

We also examined whether the chondrocyte differentiation markers (*ACAN*, *COL2A1*, and *SOX9*) are affected by Hippo signaling in 2D and 3D cultured chondrocytes. The deletion of LATS1/2 significantly decreases the *COL2A1* expression in both 2D and 3D cultures (Figures S4A and S4B). On the other hand, deletion of LATS1/2 can moderately increase the *SOX9* expression in 2D but not 3D culture, while deletion of YAP significantly increases the *SOX9* expression in both 2D and 3D culture.

In summary, our observations implicated functional interplays between biophysical microenvironment, Hippo signaling, and chondrocyte differentiation (Figures 3 and 4).

Proper regulation and activity of Hippo signaling is required for mechanoresponses of NFκB to mechanical loading

Given that Hippo signaling serves as a mechanical checkpoint and sensor of cellular homeostasis in response to biophysical environmental change, we hypothesize that deficiencies of Hippo signaling could lead to deficient mechanoresponses of chondrocytes to mechanical loading.

We first focused on whether deletion of LATS1/2 or YAP can oppositely regulate NFκB activation by mechanical loading. Unexpectedly, mechanical loading failed to induce p65 S536 phosphorylation or expression of target genes (*IL1β* and *ADAMTS4*) in LATS1/2 dKO chondrocytes (sgLATS1/2) and YAP KO (sgYAP) as in the control cells (sgCTRL) (Figures 5A and 5B).

Detailed signaling pathway analyses of mechanically loaded chondrocytes revealed that the effects of LATS1/2 or YAP gene deletion on p65 S536 phosphorylation in chondrocytes are likely independent of canonical NFκB upstream regulators (IKKα/β, IκBα) as we did not observe phosphorylation of IKKα/β and IκBα, which indicates their activity, showed a similar pattern with p65 S536 phosphorylation across different treatment or knockout groups. Interestingly, the protein level of p65 was diminished in YAP KO chondrocytes.

AP1 family members, especially cJun, are well known to functionally interact with NFκB transcriptional activation,[55] and Hippo signaling has recently been reported to tightly control c-Jun and other AP1 members in cellular acute response.[56] Therefore, we also examined c-Jun protein level and phosphorylation. However, though we observed differential c-Jun phosphorylation in LATS1/2 dKO and YAP KO cells, which is consistent with our previous report,[56] mechanical loading itself does not alter c-Jun protein level or activity (Figure 5A). This indicates that other NFκB upstream regulators are dysregulated in LATS1/2 KO and YAP KO cells. Nevertheless, our results support our notion that the core Hippo pathway components, such as LATS1/2 and YAP, are required for the NFκB regulation in chondrocytes by mechanical overloading.

LATS1/2 kinase inhibitors can be potential therapeutic agents for KOA

Based on the observation in the LATS1/2 knockout cells, we explored the potential of using LATS1/2 inhibitors to prevent the inflammatory and catabolic responses of chondrocytes to mechanical compression. We, therefore, tested a LATS1/2 small molecule inhibitor (Lats-IN-1, 10 μM), which was supplemented 18 h before exposure to a 4-h static compressive load of 20% strain. The expression of YAP/TAZ target genes (*CTGF*, *CYR61*, *AMOTL2*, and *ANKRD1*) was significantly upregulated in the compressed discs with LATS1/2 inhibitor compared to control,

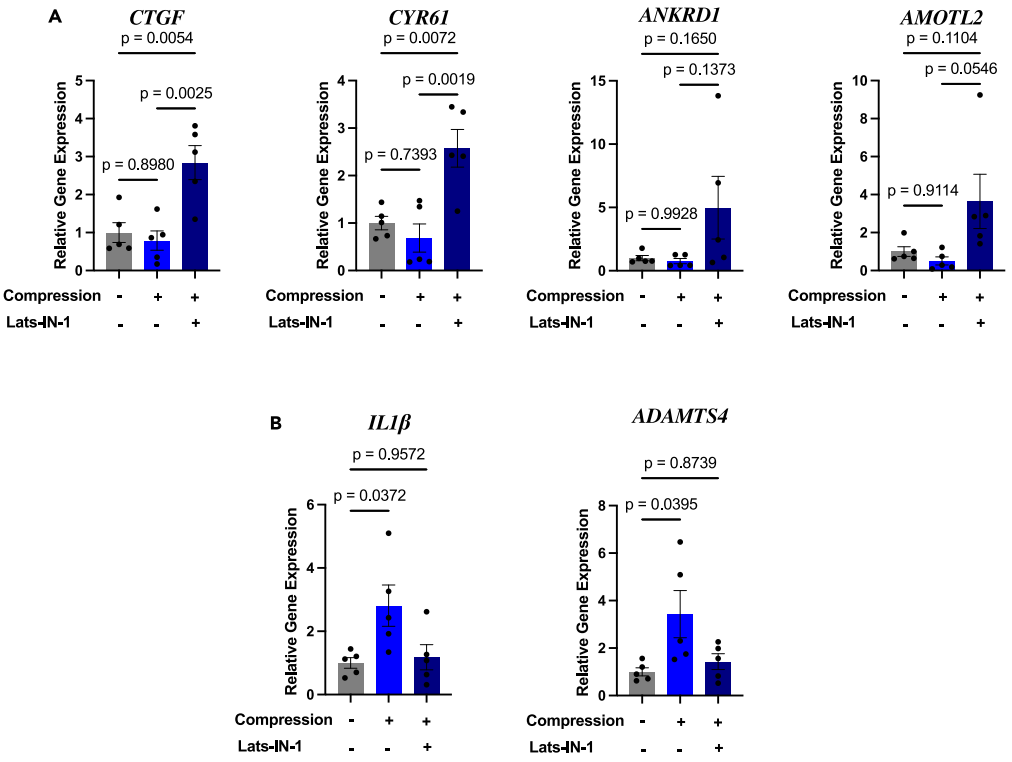

Figure 6. Effects of a LATS1/2 inhibitor, Lats-IN-1, on compressed chondrocytes

(A) The expression of YAP target genes *CTGF*, *CYR61*, *ANKRD1*, and *AMOTL2* in the chondrocytes with the LATS1/2 inhibitor Lats-IN-1 and/or compression. The data are presented as mean ± SEM.

(B) The expression of *IL1β* and *ADAMTS4* in the same set of chondrocytes. one-way ANOVA test was performed; $n = 5$.

indicating that Lats-IN-1 can effectively inhibit the activity of LATS1/2 (Figure 6A). More importantly, Lats-IN-1 suppressed upregulation of *IL1β* and *ADAMTS4* in discs subjected to mechanical load, implying that LATS1/2 inhibition can be a potential therapeutic strategy for KOA (Figure 6B), which currently lacks effective treatments.

Hippo signaling modulates the mechanoresponses of NFκB via PKC

To understand the mechanisms by which Hippo signaling controls the responses of NFκB to mechanical loading, we profiled multiple pathways that are known to be regulated by mechanical cues or control NFκB activity (Figure S5). Protein kinase A (PKA), AKT, and AMP-activated protein kinase (AMPK) are known to respond to mechanical cues, regulate chondrocyte metabolisms, and interact with NFκB.[2] We, therefore, used their phosphor-substrate antibodies to determine whether their activities are altered in LATS1/2 dKO and YAP KO cells. Mechanical compression slightly increases PKA activity in the control and LATS1/2 dKO cells, though PKA activity in the latter was high even at the basal level. In the YAP KO cells, PKA activity was downregulated by mechanical loading. Therefore, the pattern was not very consistent with NFκB activity (Figure S5A). Activities of AKT and AMPK do not correlate with NFκB activity well, either. Similarly, we did not observe activities of CDKs and ATM/ATR, which functionally interact with NFκB in various other settings,[55] correlate with NFκB activity in the chondrocytes under mechanical loading (Figure S5B). It should be emphasized that the effects of mechanical loading on these pathways were not very robust.

On the contrary, the activities of PKC in the control, LATS1/2 dKO, and YAP KO chondrocytes are similar to the patterns of NFκB (Figure 7A). The PKC activity was measured by blotting the lysates of the cells with an antibody that recognizes phospho-[(R/K)XpSX(R/K)] motif. More importantly, the mechanical load can strongly stimulate PKC activities, particularly on its substrates with a molecular weight of ~80 kDa, which likely represents the autophosphorylation of PKC (marked by *). PKC is well known to be a key regulator of NFκB in cardiomyocytes, which are also tightly regulated by mechanical loading. Multiple isoforms of PKCs regulate NFκB in both IKK-dependent and independent manners.[57] More importantly, we performed kinase enrichment analysis (KEA)[58] with the RNAseq dataset comparing preserved and damaged cartilages, discovering that activities of calcium-dependent protein kinases, which includes PKCs as a broader term, and PKC is altered in OA development (Figure S6A). In particular, atypical PKC (PKCζ) can directly phosphorylate p65 S536 and elevate p65 transcriptional activity.[59]

To determine the roles of PKCs in the mechanoregulation of NFκB, we applied a pan-PKC inhibitor sotrastaurin (AEB071) to mechanically loaded chondrocytes (Figure 7B). AEB071 can effectively block the phosphorylation of both PKC substrates and p65 S536, demonstrating that

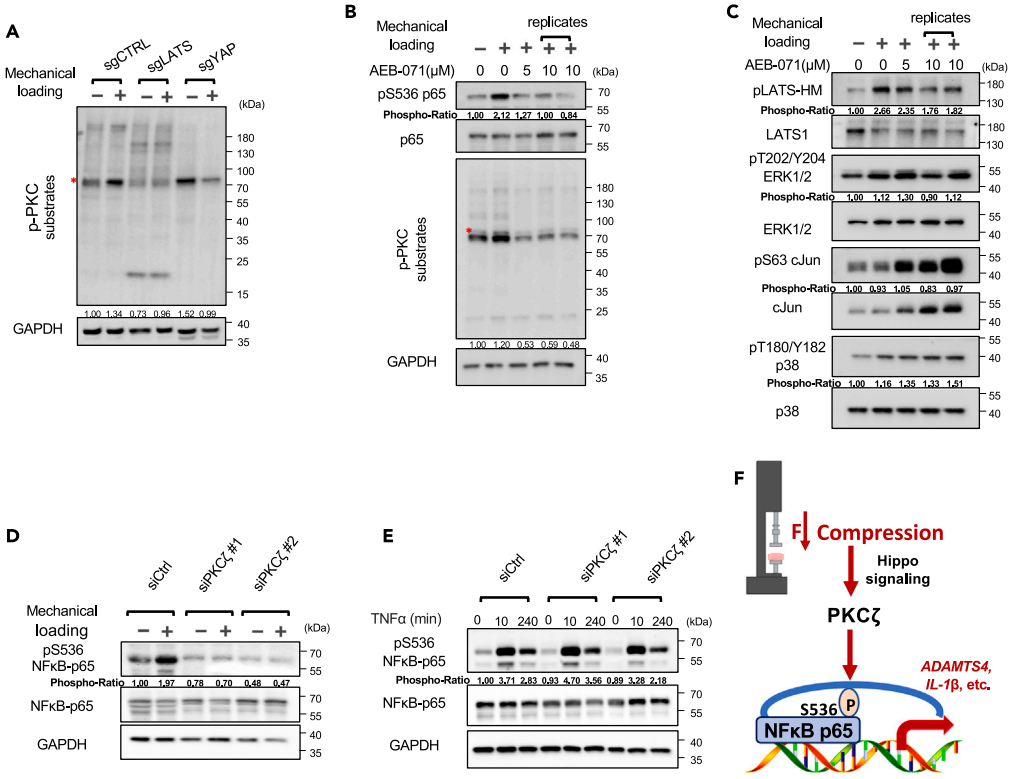

Figure 7. PKC is activated by mechanical compression in a Hippo-dependent manner and required for NFκB p65 phosphorylation at Serine 536

(A) Detection of PKC activity using phospho-PKC substrate antibodies, which targets the phospho-[(R/K)XpSX(R/K)] motif, under mechanical loading. *, indicates the predicted PKC bands.

(B) The PKC inhibitor AEB-071 blocks NFκB p65 S536 phosphorylation induced by mechanical compression.

(C) AEB-071 reduces LATS activity, as shown by the phosphorylation of the LATS hydrophobic motif.

(D) Knockdown of PKCζ with two pairs of duplex RNAi blocks NF-κB p65 S536 phosphorylation induced by mechanical compression.

(E) Knockdown of PKCζ does not affect TNFα-induced NFκB p65 S536 phosphorylation.

(F) A diagram of the proposed model in which mechanical compression activates NFκB-mediated gene transcription in a Hippo pathway-dependent manner.

PKC kinase activity is required by mechanical loading to activate NFκB. Besides NFκB, Hippo, and MAPK (ERK1/2, p38, and JNK) signaling is known to be activated by mechanical loading. We further found that AEB071 also blocked LATS phosphorylation but did not increase ERK and p38 phosphorylation, resulting from mechanical loading (Figure 7C).

We subsequently knocked down PKCζ, using RNA interference, to determine whether this atypical PKC is the key player in the NFκB regulation in chondrocytes by mechanical loading. We transfected two pairs of duplex RNAi oligos targeting PKCζ into chondrocytes, both of which resulted in efficient PKCζ knockdown (Figure S6B). Both pairs of PKCζ RNAi nearly blocked all p65 S536 phosphorylation caused by mechanical loading, proving an indispensable role of PKCζ in mechanoinflammation (Figure 7D). Furthermore, the NFκB regulator role of PKCζ is rather specific to mechanical loading, as PKCζ knockdown failed to block TNF-induced p65 S536 phosphorylation in chondrocytes (Figure 7E). We also observed that overexpression of Hippo kinases MST2 and LATS1 cannot directly increase p65 S536 phosphorylation regardless of the PKCζ expression (Figure S6C). This indicates that other mechanisms are needed, in collaboration with Hippo signaling, to activate NFκB in chondrocytes upon mechanical compression.

DISCUSSION

Modeling of mechanical overload-induced KOA

We have developed an *in vitro* bioengineering model to study mechanotransduction signaling and transcriptome using a 4 h 20% compression loading regimen. Our model has successfully recapitulated the mechanoregulation of NFκB and subsequent target gene expression upon mechanical compressional loading.

Several studies have quantified *in vivo* strain levels to determine normal ranges of compression in human knee cartilage. *Eckstein* et al. used MRI and 3D image analysis to show the strain levels during typical activities, such as knee bending, jumping, and static exercise, are within the range of 2%–10% using MRI evaluation and 3D image analysis.[60] Previous MRI studies have shown that cartilage deformation in knees increases with a higher BMI[61] and is greater in osteoarthritic knees than in healthy knees.[62] Furthermore, it was found that 20% static

compression for 4 h resulted in a transient increase in chondrocyte's *ADAMTS4* expression, and a 10% strain was modeled as a normal strain showing no effects on gene expression.[29]

Nevertheless, we have been using conventional cell culture medium and atmospheric conditions, which are rather different from the nutrient and oxygen levels in normal articular cartilage. As mechanosensing pathways, such as Hippo and NFκB signaling, incorporate biochemical cues for cellular homeostasis, therefore we will further optimize our system using a human plasma-like medium and more advanced cell culture incubator with oxygen and hydrostatic pressure control.[63]

Since dynamic loading at low magnitude can suppress the *IL1β*-mediated catabolic responses of chondrocytes,[64–67] dynamic compression studies utilizing a similar protocol could also provide important findings to evaluate the involvement of the Hippo pathway under different loading conditions, which may recapitulate physiologic environments more realistically. Other loading factors, including loading duration, magnitude, and frequency, should also be further defined. Furthermore, compression rate, or how quickly a load is applied to the disk, is another essential topic to investigate in future approaches, as high-rate impacts can potentially lead to post-traumatic KOA. Thus, evaluating the Hippo pathway with various loading rates may provide highly valuable insight.[68]

The functional interplay of NFκB and Hippo signaling in chondrocyte mechanoresponses

Several studies have investigated the function of the Hippo pathway and YAP/TAZ functionality in articular cartilage homeostasis of knee chondrocytes. Central to the Hippo pathway is the kinase LATS1/2, which functions to phosphorylate YAP/TAZ and inhibit nuclear translocation.[19] This state of cytoplasmic YAP/TAZ sequestration is referred to as the active state of the Hippo pathway. When the Hippo pathway is inactive, YAP can freely translocate into the nucleus and has been associated with the preservation of articular cartilage integrity specifically via direct interaction with TAK1 and attenuation of the NFκB signaling cascade in an OA mouse model.[19] The attenuation of NFκB is key to modulating inflammatory pathways associated with OA. In a study by *Yan* et al., using a nanoparticle-based siRNA, NFκB was suppressed and resulted in reduced chondrocyte death and cartilage degeneration.[69] One study found that YAP is notably activated during the development of OA in mice.[20] The targeted removal of YAP in mouse chondrocytes (conditional knockout or cKO) showed preservation of collagen II expression, a key component of cartilage, thus preventing cartilage degradation in that OA model. Additionally, the introduction of a YAP-specific inhibitor, Verteporfin, through injections directly into the joint, significantly aided in maintaining the balance of cartilage in the OA mouse model.[20] These apparently conflicting results implied a context-dependent, but very crucial, role of YAP and/or Hippo signaling in OA and NFκB regulation.

Our results have helped reconcile these studies in the mechanobiology settings. We showed that either full inactivation of Hippo signaling (full YAP activation) or complete inactivation of YAP can block NF-κB p65 S536 phosphorylation and target gene expression (Figure 5). These findings suggest that the full cycle of YAP phosphorylation-dephosphorylation by the Hippo kinase cascade is essential for chondrocyte mechanoresponses, as illustrated in Figure 7F. In future, it is important to understand how deletion of YAP in chondrocytes reduced NFκB p65 expression, either at transcription or post-transcription levels. Functionally, the decreased p65 expression in YAP KO chondrocytes may reflect the adaption of chondrocytes to the complete loss of YAP proteins (Figure 5A). The mechanoinflammatory pathways are rewired when key players, such as YAP, are removed from chondrocytes. This may be in part due to various positive and negative feedbacks of Hippo pathway regulation that have been summarized previously.[21]

The notion that proper Hippo-YAP regulation and basal YAP activity are required for mechanoinflammation is further supported by the mechanoresponses of PKC and PKA in chondrocytes (Figures 7 and S5A). Therefore, blocking this Hippo phosphorylation cycle is a potential strategy to mitigate cartilage degradation, as supported by our studies with LATS1/2 inhibitor LATS-IN-1 and PKC inhibitor AEB-071 (Figures 6B and 7B).

On the other hand, compared with OA mouse surgery models, anterior aruciate ligament transection or destabilization of the medial meniscus surgeries used in a previous study,[19] our model is focused on the aspect of mechanical overloading during OA model development. Our model allows us to study the direct cellular response of chondrocytes to mechanical stimuli in a simplified environment, without the involvement of inflammatory cells and other players. More importantly, our study focuses on the immediate responses to mechanical loading, while the mouse models better recapitulate the accumulative effects of aberrant force distribution to joints. Our model may better serve for the study of post-traumatic OA, caused by insults to the joint from an external mechanical force, which results in injuries to the articular cartilage.

Characterization of mechanotransduction signaling cascades

Our study has opened a new avenue for identifying and characterizing novel components of mechanotransduction signaling cascades. There are several key mechanism questions to investigate in the next. First, it is worth investigating which PKC isoform(s) responds to mechanical overloading and how mechanical overloading and Hippo signaling regulate the PKC(s). Second, two reports have introduced opposite roles of conventional, novel, and atypical PKCs in Hippo signaling.[70,71] However, it is unknown how Hippo signaling can in turn regulate PKCs. Our study is therefore the first report showing that Hippo signaling can regulate PKCs in mechanically loaded cells. Third, conventional, novel, and atypical PKCs can sense various secondary messengers and phosphoinositol.[72] Therefore, investigating the functional interactions between PKC and Hippo will likely improve our fundamental understanding of how mechanical loading is sensed at the plasma membrane level and subsequently propagated into biochemical signals that eventually alter chondrocyte transcriptomes. Hippo signaling may crosstalk with PKCζ upstream effectors, such as PDK1 and PI3K, as previous studies[73,74] already showed the interplay of YAP and AKT, another downstream effector PDK1 and PI3K.

In conclusion, the results presented in the current study suggest that the interplay of NFκB, Hippo, and PKC signaling may be a modifiable target in the response of chondrocytes under mechanical loading, and in a broader context, the response of chondrocytes in patients with KOA. Kinase inhibitors, such as PKC inhibitor AEB-071, which are currently being tested in clinical trials for other diseases (i.e., uveal melanoma), may apply to OA by blocking inflammation and preventing disease progression.

Limitations of the study

Though our model could provide more mechanistic insights for signaling studies, the limitation is that it may not fully reflect how chondrocytes, when interacting with other joint cells and matrix, respond to mechanical compression. Future studies with co-culture chondrocytes and other joint cells will provide better systems for mechanistic studies. A recent study[52] showed that dynamic tensile loading exhibits anti-inflammatory effects on chondrocytes via YAP activation. A comparison of physiological and pathological loading conditions, both static and dynamic, will help us better understand the mechanoresponses of chondrocytes and how they contribute to disease initiation.

STAR★METHODS

Detailed methods are provided in the online version of this paper and include the following:

- KEY RESOURCES TABLE
- RESOURCE AVAILABILITY
  - Lead contact
  - Materials availability
  - Data and code availability
- EXPERIMENTAL MODEL AND STUDY PARTICIPANT DETAILS
  - Preparation of 3-dimensional chondrocyte-agarose constructs
  - 2D static compression
  - 3D static compression
- METHOD DETAILS
  - Quantitative real-time PCR
  - CRISPR/Cas9 gene deletion in chondrocytes
  - RNA interference in chondrocytes
  - Plasmids co-transfection in chondrocytes
  - Western blot analysis
  - Polyacrylamide hydrogel substrate
  - Bioinformatic analysis
- QUANTIFICATION AND STATISTICAL ANALYSIS
  - Statistical analysis

SUPPLEMENTAL INFORMATION

Supplemental information can be found online at https://doi.org/10.1016/j.isci.2024.109983.

ACKNOWLEDGMENTS

C.W., O.F.P., and Q.T.E were supported by the USOAR scholarship from the University of Miami Miller School of Medicine. Z.M. is supported by the National Institute of General Medical Sciences of the National Institutes of Health (NIH) under award number R35GM142504. C.W. is in part supported by a postdoc trainee award from the Sylvester Comprehensive Cancer Center TB-TRO-2024-02.

AUTHOR CONTRIBUTIONS

Z.M. and C.-Y. H. conceived the project, obtained the funding for the project, and supervised the study. X.C. generated CRISPR knockout cells. X.C. Y. W., C.W., and C. D.R performed biochemical analyses. C.W., O.F.P., L.H., C.F., and Q.T.E. performed the compression experiments. X.C., C.W., O.F.P., T.M.B., C.-Y.H., and Z.M. wrote the manuscript. L.K. and T.M.B. provided intellectual support.

DECLARATION OF INTERESTS

The authors declare no competing interests.

Received: November 6, 2023
Revised: March 4, 2024
Accepted: May 13, 2024
Published: May 15, 2024

REFERENCES

1. Martel-Pelletier, J., Barr, A.J., Cicuttini, F.M., Conaghan, P.G., Cooper, C., Goldring, M.B., Goldring, S.R., Jones, G., Teichtahl, A.J., and Pelletier, J.P. (2016). Osteoarthritis. Nat. Rev. Dis. Primers *2*, 16072. https://doi.org/10.1038/nrdp.2016.72.
2. Latourte, A., Kloppenburg, M., and Richette, P. (2020). Emerging pharmaceutical therapies for osteoarthritis. Nat. Rev. Rheumatol. *16*, 673–688. https://doi.org/10.1038/s41584-020-00518-6.
3. Buckwalter, J.A., Anderson, D.D., Brown, T.D., Tochigi, Y., and Martin, J.A. (2013). The Roles of Mechanical Stresses in the Pathogenesis of Osteoarthritis: Implications for Treatment of Joint Injuries. Cartilage *4*, 286–294. https://doi.org/10.1177/1947603513495889.
4. Anderson, D.D., Chubinskaya, S., Guilak, F., Martin, J.A., Oegema, T.R., Olson, S.A., and Buckwalter, J.A. (2011). Post-traumatic osteoarthritis: improved understanding and opportunities for early intervention. J. Orthop. Res. *29*, 802–809. https://doi.org/10.1002/jor.21359.
5. Vincent, T.L. (2013). Targeting mechanotransduction pathways in osteoarthritis: a focus on the pericellular matrix. Curr. Opin. Pharmacol. *13*, 449–454. https://doi.org/10.1016/j.coph.2013.01.010.
6. Batushansky, A., Zhu, S., Komaravolu, R.K., South, S., Mehta-D'souza, P., and Griffin, T.M. (2022). Fundamentals of OA. An initiative of Osteoarthritis and Cartilage. Obesity and metabolic factors in OA. Osteoarthritis Cartilage *30*, 501–515. https://doi.org/10.1016/j.joca.2021.06.013.
7. Leong, D.J., Hardin, J.A., Cobelli, N.J., and Sun, H.B. (2011). Mechanotransduction and cartilage integrity. Ann. N. Y. Acad. Sci. *1240*, 32–37. https://doi.org/10.1111/j.1749-6632.2011.06301.x.
8. Oliveira, S., Andrade, R., Silva, F.S., Espregueira-Mendes, J., Hinckel, B.B., Leal, A., and Carvalho, Ó. (2023). Effects and mechanotransduction pathways of therapeutic ultrasound on healthy and osteoarthritic chondrocytes: a systematic review of *in vitro* studies. Osteoarthritis Cartilage *31*, 317–339. https://doi.org/10.1016/j.joca.2022.07.014.
9. Zignego, D.L., Hilmer, J.K., Bothner, B., Schell, W.J., and June, R.K. (2019). Primary human chondrocytes respond to compression with phosphoproteomic signatures that include microtubule activation. J. Biomech. *97*, 109367. https://doi.org/10.1016/j.jbiomech.2019.109367.
10. Zhao, Z., Li, Y., Wang, M., Zhao, S., Zhao, Z., and Fang, J. (2020). Mechanotransduction pathways in the regulation of cartilage chondrocyte homoeostasis. J. Cell Mol. Med. *24*, 5408–5419. https://doi.org/10.1111/jcmm.15204.
11. Sophia Fox, A.J., Bedi, A., and Rodeo, S.A. (2009). The basic science of articular cartilage: structure, composition, and function. Sports Health *1*, 461–468. https://doi.org/10.1177/1941738109350438.
12. Zhu, J., Zhu, Y., Xiao, W., Hu, Y., and Li, Y. (2020). Instability and excessive mechanical loading mediate subchondral bone changes to induce osteoarthritis. Ann. Transl. Med. *8*, 350. https://doi.org/10.21037/atm.2020.02.103.
13. Sanchez-Adams, J., Leddy, H.A., McNulty, A.L., O'Conor, C.J., and Guilak, F. (2014). The mechanobiology of articular cartilage: bearing the burden of osteoarthritis. Curr. Rheumatol. Rep. *16*, 451. https://doi.org/10.1007/s11926-014-0451-6.
14. Kurz, B., Lemke, A.K., Fay, J., Pufe, T., Grodzinsky, A.J., and Schünke, M. (2005). Pathomechanisms of cartilage destruction by mechanical injury. Ann. Anat. *187*, 473–485. https://doi.org/10.1016/j.aanat.2005.07.003.
15. Pan, D. (2010). The hippo signaling pathway in development and cancer. Dev. Cell *19*, 491–505. https://doi.org/10.1016/j.devcel.2010.09.011.
16. Meng, Z., Qiu, Y., Lin, K.C., Kumar, A., Placone, J.K., Fang, C., Wang, K.C., Lu, S., Pan, M., Hong, A.W., et al. (2018). RAP2 mediates mechanoresponses of the Hippo pathway. Nature *560*, 655–660. https://doi.org/10.1038/s41586-018-0444-0.
17. Moya, I.M., and Halder, G. (2019). Hippo-YAP/TAZ signalling in organ regeneration and regenerative medicine. Nat. Rev. Mol. Cell Biol. *20*, 211–226. https://doi.org/10.1038/s41580-018-0086-y.
18. Dey, A., Varelas, X., and Guan, K.L. (2020). Targeting the Hippo pathway in cancer, fibrosis, wound healing and regenerative medicine. Nat. Rev. Drug Discov. *19*, 480–494. https://doi.org/10.1038/s41573-020-0070-z.
19. Deng, Y., Lu, J., Li, W., Wu, A., Zhang, X., Tong, W., Ho, K.K., Qin, L., Song, H., and Mak, K.K. (2018). Reciprocal inhibition of YAP/TAZ and NF-kappaB regulates osteoarthritic cartilage degradation. Nat. Commun. *9*, 4564. https://doi.org/10.1038/s41467-018-07022-2.
20. Zhang, X., Cai, D., Zhou, F., Yu, J., Wu, X., Yu, D., Zou, Y., Hong, Y., Yuan, C., Chen, Y., et al. (2020). Targeting downstream subcellular YAP activity as a function of matrix stiffness with Verteporfin-encapsulated chitosan microsphere attenuates osteoarthritis. Biomaterials *232*, 119724. https://doi.org/10.1016/j.biomaterials.2019.119724.
21. Meng, Z., Moroishi, T., and Guan, K.L. (2016). Mechanisms of Hippo pathway regulation. Genes Dev. *30*, 1–17. https://doi.org/10.1101/gad.274027.115.
22. Cai, X., Wang, K.C., and Meng, Z. (2021). Mechanoregulation of YAP and TAZ in Cellular Homeostasis and Disease Progression. Front. Cell Dev. Biol. *9*, 673599. https://doi.org/10.3389/fcell.2021.673599.
23. Meng, Z., Li, F.L., Fang, C., Yeoman, B., Qiu, Y., Wang, Y., Cai, X., Lin, K.C., Yang, D., Luo, M., et al. (2022). The Hippo pathway mediates Semaphorin signaling. Sci. Adv. *8*, eabl9806. https://doi.org/10.1126/sciadv.abl9806.
24. Wang, N., Zhang, X., Rothrauff, B.B., Fritch, M.R., Chang, A., He, Y., Yeung, M., Liu, S., Lipa, K.E., Lei, G., et al. (2022). Novel role of estrogen receptor-alpha on regulating chondrocyte phenotype and response to mechanical loading. Osteoarthritis Cartilage *30*, 302–314. https://doi.org/10.1016/j.joca.2021.11.002.
25. Verma, P., and Dalal, K. (2011). ADAMTS-4 and ADAMTS-5: key enzymes in osteoarthritis. J. Cell. Biochem. *112*, 3507–3514. https://doi.org/10.1002/jcb.23298.
26. Vincent, T.L. (2019). IL-1 in osteoarthritis: time for a critical review of the literature. F1000Res. *8*. F1000 Faculty Rev-934. https://doi.org/10.12688/f1000research.18831.1.
27. Tse, J.M., Cheng, G., Tyrrell, J.A., Wilcox-Adelman, S.A., Boucher, Y., Jain, R.K., and Munn, L.L. (2012). Mechanical compression drives cancer cells toward invasive phenotype. Proc. Natl. Acad. Sci. USA *109*, 911–916. https://doi.org/10.1073/pnas.1118910109.
28. Li, Y., Li, Y., Zhang, Q., Wang, L., Guo, M., Wu, X., Guo, Y., Chen, J., and Chen, W. (2019). Mechanical Properties of Chondrocytes Estimated from Different Models of Micropipette Aspiration. Biophys. J. *116*, 2181–2194. https://doi.org/10.1016/j.bpj.2019.04.022.
29. Fitzgerald, J.B., Jin, M., Dean, D., Wood, D.J., Zheng, M.H., and Grodzinsky, A.J. (2004). Mechanical compression of cartilage explants induces multiple time-dependent gene expression patterns and involves intracellular calcium and cyclic AMP. J. Biol. Chem. *279*, 19502–19511. https://doi.org/10.1074/jbc.M400437200.
30. Rigoglou, S., and Papavassiliou, A.G. (2013). The NF-kappaB signalling pathway in osteoarthritis. Int. J. Biochem. Cell Biol. *45*, 2580–2584. https://doi.org/10.1016/j.biocel.2013.08.018.
31. Cogswell, J.P., Godlevski, M.M., Wisely, G.B., Clay, W.C., Leesnitzer, L.M., Ways, J.P., and Gray, J.G. (1994). NF-kappa B regulates IL-1 beta transcription through a consensus NF-kappa B binding site and a nonconsensus CRE-like site. J. Immunol. *153*, 712–723.
32. Tian, Y., Yuan, W., Fujita, N., Wang, J., Wang, H., Shapiro, I.M., and Risbud, M.V. (2013). Inflammatory cytokines associated with degenerative disc disease control aggrecanase-1 (ADAMTS-4) expression in nucleus pulposus cells through MAPK and NF-kappaB. Am. J. Pathol. *182*, 2310–2321. https://doi.org/10.1016/j.ajpath.2013.02.037.
33. Chang, S.H., Mori, D., Kobayashi, H., Mori, Y., Nakamoto, H., Okada, K., Taniguchi, Y., Sugita, S., Yano, F., Chung, U.I., et al. (2019). Excessive mechanical loading promotes osteoarthritis through the gremlin-1-NF-kappaB pathway. Nat. Commun. *10*, 1442. https://doi.org/10.1038/s41467-019-09491-5.
34. Kumar, A., and Boriek, A.M. (2003). Mechanical stress activates the nuclear factor-kappaB pathway in skeletal muscle fibers: a possible role in Duchenne muscular dystrophy. Faseb. J. *17*, 386–396. https://doi.org/10.1096/fj.02-0542com.
35. Sasaki, C.Y., Barberi, T.J., Ghosh, P., and Longo, D.L. (2005). Phosphorylation of RelA/p65 on serine 536 defines an IkappaBalpha-independent NF-kappaB pathway. J. Biol. Chem. *280*, 34538–34547. https://doi.org/10.1074/jbc.M504943200.
36. Sakurai, H., Chiba, H., Miyoshi, H., Sugita, T., and Toriumi, W. (1999). IkappaB kinases phosphorylate NF-kappaB p65 subunit on serine 536 in the transactivation domain. J. Biol. Chem. *274*, 30353–30356. https://doi.org/10.1074/jbc.274.43.30353.
37. Taniguchi, K., and Karin, M. (2018). NF-kappaB, inflammation, immunity and cancer: coming of age. Nat. Rev. Immunol. *18*, 309–324. https://doi.org/10.1038/nri.2017.142.
38. Taylor, R.C., Cullen, S.P., and Martin, S.J. (2008). Apoptosis: controlled demolition at the cellular level. Nat. Rev. Mol. Cell Biol. *9*, 231–241. https://doi.org/10.1038/nrm2312.
39. Dikic, I., and Elazar, Z. (2018). Mechanism and medical implications of mammalian autophagy. Nat. Rev. Mol. Cell Biol. *19*, 349–364. https://doi.org/10.1038/s41580-018-0003-4.

40. Vandenabeele, P., Galluzzi, L., Vanden Berghe, T., and Kroemer, G. (2010). Molecular mechanisms of necroptosis: an ordered cellular explosion. Nat. Rev. Mol. Cell Biol. *11*, 700–714. https://doi.org/10.1038/nrm2970.
41. You, J.S., McNally, R.M., Jacobs, B.L., Privett, R.E., Gundermann, D.M., Lin, K.H., Steinert, N.D., Goodman, C.A., and Hornberger, T.A. (2019). The role of raptor in the mechanical load-induced regulation of mTOR signaling, protein synthesis, and skeletal muscle hypertrophy. Faseb. J. *33*, 4021–4034. https://doi.org/10.1096/fj.201801653RR.
42. Guan, Y., Yang, X., Yang, W., Charbonneau, C., and Chen, Q. (2014). Mechanical activation of mammalian target of rapamycin pathway is required for cartilage development. FASEB J *28*, 4470–4481. https://doi.org/10.1096/fj.14-252783.
43. Fernando, H.N., Czamanski, J., Yuan, T.Y., Gu, W., Salahadin, A., and Huang, C.Y.C. (2011). Mechanical loading affects the energy metabolism of intervertebral disc cells. J. Orthop. Res. *29*, 1634–1641.
44. Hubka, K.M., Dahlin, R.L., Meretoja, V.V., Kasper, F.K., and Mikos, A.G. (2014). Enhancing chondrogenic phenotype for cartilage tissue engineering: monoculture and coculture of articular chondrocytes and mesenchymal stem cells. Tissue Eng. Part B Rev. *20*, 641–654. https://doi.org/10.1089/ten.TEB.2014.0034.
45. Rim, Y.A., Nam, Y., and Ju, J.H. (2020). The Role of Chondrocyte Hypertrophy and Senescence in Osteoarthritis Initiation and Progression. Int. J. Mol. Sci. *21*, 2358. https://doi.org/10.3390/ijms21072358.
46. Hallstrom, G.F., Jones, D.L., Locke, R.C., Bonnevie, E.D., Kim, S.Y., Laforest, L., Garcia, D.C., and Mauck, R.L. (2023). Microenvironmental mechanoactivation through Yap/Taz suppresses chondrogenic gene expression. Mol. Biol. Cell *34*, ar73. https://doi.org/10.1091/mbc.E22-12-0543.
47. Wu, X., Su, J., Wei, J., Jiang, N., and Ge, X. (2021). Recent Advances in Three-Dimensional Stem Cell Culture Systems and Applications. Stem Cells Int. *2021*, 9477332. https://doi.org/10.1155/2021/9477332.
48. Zhao, B., Li, L., Wang, L., Wang, C.Y., Yu, J., and Guan, K.L. (2012). Cell detachment activates the Hippo pathway via cytoskeleton reorganization to induce anoikis. Genes Dev. *26*, 54–68. https://doi.org/10.1101/gad.173435.111.
49. Park, S.-J., Goodman, M.B., and Pruitt, B.L. (2005). Measurement of mechanical properties of Caenorhabditis elegans with a piezoresistive microcantilever system. In 3rd IEEE/EMBS Special Topic Conference on Microtechnology in Medicine and Biology. https://doi.org/10.1109/MMB.2005.1548488.
50. Qi, H., Zhang, Y., Xu, L., Zheng, X., Li, Y., Wei, Q., Li, Y., Zhao, Z., and Fang, J. (2023). Loss of RAP2A Aggravates Cartilage Degradation in TMJOA via YAP Signaling. J. Dent. Res. *102*, 302–312. https://doi.org/10.1177/00220345221132213.
51. Zhu, J., Lun, W., Feng, Q., Cao, X., and Li, Q. (2023). Mesenchymal stromal cells modulate YAP by verteporfin to mimic cartilage development and construct cartilage organoids based on decellularized matrix scaffolds. J. Mater. Chem. B *11*, 7442–7453. https://doi.org/10.1039/d3tb01114c.
52. Meng, H., Fu, S., Ferreira, M.B., Hou, Y., Pearce, O.M., Gavara, N., and Knight, M.M. (2023). YAP activation inhibits inflammatory signalling and cartilage breakdown associated with reduced primary cilia expression. Osteoarthritis Cartilage *31*, 600–612. https://doi.org/10.1016/j.joca.2022.11.001.
53. Meng, Z., Moroishi, T., Mottier-Pavie, V., Plouffe, S.W., Hansen, C.G., Hong, A.W., Park, H.W., Mo, J.S., Lu, W., Lu, S., et al. (2015). MAP4K family kinases act in parallel to MST1/2 to activate LATS1/2 in the Hippo pathway. Nat. Commun. *6*, 8357. https://doi.org/10.1038/ncomms9357.
54. Dupont, S., Morsut, L., Aragona, M., Enzo, E., Giulitti, S., Cordenonsi, M., Zanconato, F., Le Digabel, J., Forcato, M., Bicciato, S., et al. (2011). Role of YAP/TAZ in mechanotransduction. Nature *474*, 179–183. https://doi.org/10.1038/nature10137.
55. Oeckinghaus, A., Hayden, M.S., and Ghosh, S. (2011). Crosstalk in NF-kappaB signaling pathways. Nat. Immunol. *12*, 695–708. https://doi.org/10.1038/ni.2065.
56. Koo, J.H., Plouffe, S.W., Meng, Z., Lee, D.H., Yang, D., Lim, D.S., Wang, C.Y., and Guan, K.L. (2020). Induction of AP-1 by YAP/TAZ contributes to cell proliferation and organ growth. Genes Dev. *34*, 72–86. https://doi.org/10.1101/gad.331546.119.
57. Abe, J.I. (2007). Role of PKCs and NF-kappaB activation in myocardial inflammation: enemy or ally? J. Mol. Cell. Cardiol. *43*, 404–408. https://doi.org/10.1016/j.yjmcc.2007.07.002.
58. Kuleshov, M.V., Xie, Z., London, A.B.K., Yang, J., Evangelista, J.E., Lachmann, A., Shu, I., Torre, D., and Ma'ayan, A. (2021). KEA3: improved kinase enrichment analysis via data integration. Nucleic Acids Res. *49*, W304–W316. https://doi.org/10.1093/nar/gkab359.
59. Diaz-Meco, M.T., and Moscat, J. (2012). The atypical PKCs in inflammation: NF-kappaB and beyond. Immunol. Rev. *246*, 154–167. https://doi.org/10.1111/j.1600-065X.2012.01093.x.
60. Eckstein, F., Hudelmaier, M., and Putz, R. (2006). The effects of exercise on human articular cartilage. J. Anat. *208*, 491–512. https://doi.org/10.1111/j.1469-7580.2006.00546.x.
61. Collins, A.T., Kulvaranon, M.L., Cutcliffe, H.C., Utturkar, G.M., Smith, W.A.R., Spritzer, C.E., Guilak, F., and DeFrate, L.E. (2018). Obesity alters the *in vivo* mechanical response and biochemical properties of cartilage as measured by MRI. Arthritis Res. Ther. *20*, 232. https://doi.org/10.1186/s13075-018-1727-4.
62. Cotofana, S., Eckstein, F., Wirth, W., Souza, R.B., Li, X., Wyman, B., Hellio-Le Graverand, M.P., Link, T., and Majumdar, S. (2011). In vivo measures of cartilage deformation: patterns in healthy and osteoarthritic female knees using 3T MR imaging. Eur. Radiol. *21*, 1127–1135. https://doi.org/10.1007/s00330-011-2057-y.
63. Cantor, J.R., Abu-Remaileh, M., Kanarek, N., Freinkman, E., Gao, X., Louissaint, A., Jr., Lewis, C.A., and Sabatini, D.M. (2017). Physiologic Medium Rewires Cellular Metabolism and Reveals Uric Acid as an Endogenous Inhibitor of UMP Synthase. Cell *169*, 258–272.e17. https://doi.org/10.1016/j.cell.2017.03.023.
64. Vernon, L., Abadin, A., Wilensky, D., Huang, C.Y.C., and Kaplan, L. (2014). Subphysiological compressive loading reduces apoptosis following acute impact injury in a porcine cartilage model. Sports Health *6*, 81–88. https://doi.org/10.1177/1941738113504379.
65. Li, Y., Frank, E.H., Wang, Y., Chubinskaya, S., Huang, H.H., and Grodzinsky, A.J. (2013). Moderate dynamic compression inhibits pro-catabolic response of cartilage to mechanical injury, tumor necrosis factor-α and interleukin-6, but accentuates degradation above a strain threshold. Osteoarthritis Cartilage *21*, 1933–1941. https://doi.org/10.1016/j.joca.2013.08.021.
66. Torzilli, P.A., Bhargava, M., Park, S., and Chen, C.T.C. (2010). Mechanical load inhibits IL-1 induced matrix degradation in articular cartilage. Osteoarthritis Cartilage *18*, 97–105. https://doi.org/10.1016/j.joca.2009.07.012.
67. Hazbun, L., Martinez, J.A., Best, T.M., Kaplan, L., and Huang, C.Y. (2021). Anti-inflammatory effects of tibial axial loading on knee articular cartilage post traumatic injury. J. Biomech. *128*, 110736. https://doi.org/10.1016/j.jbiomech.2021.110736.
68. Argote, P.F., Kaplan, J.T., Poon, A., Xu, X., Cai, L., Emery, N.C., Pierce, D.M., and Neu, C.P. (2019). Chondrocyte viability is lost during high-rate impact loading by transfer of amplified strain, but not stress, to pericellular and cellular regions. Osteoarthritis Cartilage *27*, 1822–1830. https://doi.org/10.1016/j.joca.2019.07.018.
69. Yan, H., Duan, X., Pan, H., Holguin, N., Rai, M.F., Akk, A., Springer, L.E., Wickline, S.A., Sandell, L.J., and Pham, C.T.N. (2016). Suppression of NF-kappaB activity via nanoparticle-based siRNA delivery alters early cartilage responses to injury. Proc. Natl. Acad. Sci. USA *113*, E6199–E6208. https://doi.org/10.1073/pnas.1608245113.
70. Gong, R., Hong, A.W., Plouffe, S.W., Zhao, B., Liu, G., Yu, F.X., Xu, Y., and Guan, K.L. (2015). Opposing roles of conventional and novel PKC isoforms in Hippo-YAP pathway regulation. Cell Res. *25*, 985–988. https://doi.org/10.1038/cr.2015.88.
71. Archibald, A., Al-Masri, M., Liew-Spilger, A., and McCaffrey, L. (2015). Atypical protein kinase C induces cell transformation by disrupting Hippo/Yap signaling. Mol. Biol. Cell *26*, 3578–3595. https://doi.org/10.1091/mbc.E15-05-0265.
72. Parker, P.J., Brown, S.J., Calleja, V., Chakravarty, P., Cobbaut, M., Linch, M., Marshall, J.J.T., Martini, S., McDonald, N.Q., Soliman, T., and Watson, L. (2021). Equivocal, explicit and emergent actions of PKC isoforms in cancer. Nat. Rev. Cancer *21*, 51–63. https://doi.org/10.1038/s41568-020-00310-4.
73. Lin, Z., Zhou, P., von Gise, A., Gu, F., Ma, Q., Chen, J., Guo, H., van Gorp, P.R.R., Wang, D.Z., and Pu, W.T. (2015). Pi3kcb links Hippo-YAP and PI3K-AKT signaling pathways to promote cardiomyocyte proliferation and survival. Circ. Res. *116*, 35–45. https://doi.org/10.1161/CIRCRESAHA.115.304457.
74. Borreguero-Munoz, N., Fletcher, G.C., Aguilar-Aragon, M., Elbediwy, A., Vincent-Mistiaen, Z.I., and Thompson, B.J. (2019). The Hippo pathway integrates PI3K-Akt signals with mechanical and polarity cues to control tissue growth. PLoS Biol. *17*, e3000509. https://doi.org/10.1371/journal.pbio.3000509.
75. Yin, X., Motorwala, A., Vesvoranan, O., Levene, H.B., Gu, W., and Huang, C.Y. (2020). Effects of Glucose Deprivation on ATP and Proteoglycan Production of Intervertebral Disc Cells under Hypoxia. Sci. Rep. *10*, 8899.

https://doi.org/10.1038/s41598-020-65691-w.

76. Ogura, T., Tsuchiya, A., Minas, T., and Mizuno, S. (2015). Methods of high integrity RNA extraction from cell/agarose construct. BMC Res. Notes *8*, 644. https://doi.org/10.1186/s13104-015-1627-5.
77. Livak, K.J., and Schmittgen, T.D. (2001). Analysis of relative gene expression data using real-time quantitative PCR and the 2(-Delta Delta C(T)) Method. Methods *25*, 402–408. https://doi.org/10.1006/meth.2001.1262.
78. Tse, J.R., and Engler, A.J. (2010). Preparation of hydrogel substrates with tunable mechanical properties. Curr. Protoc. Cell Biol. *Chapter 10*. Unit 10.16. https://doi.org/10.1002/0471143030.cb1016s47.
79. Love, M.I., Huber, W., and Anders, S. (2014). Moderated estimation of fold change and dispersion for RNA-seq data with DESeq2. Genome Biol. *15*, 550. https://doi.org/10.1186/s13059-014-0550-8.
80. Subramanian, A., Tamayo, P., Mootha, V.K., Mukherjee, S., Ebert, B.L., Gillette, M.A., Paulovich, A., Pomeroy, S.L., Golub, T.R., Lander, E.S., and Mesirov, J.P. (2005). Gene set enrichment analysis: A knowledge-based approach for interpreting genome-wide expression profiles. Proc. Natl. Acad. Sci. USA *102*, 15545–15550. https://doi.org/10.1073/pnas.0506580102.
81. Keenan, A.B., Torre, D., Lachmann, A., Leong, A.K., Wojciechowicz, M.L., Utti, V., Jagodnik, K.M., Kropiwnicki, E., Wang, Z., and Ma'ayan, A. (2019). ChEA3: transcription factor enrichment analysis by orthogonal omics integration. Nucleic Acids Res. *47*, W212–W224. https://doi.org/10.1093/nar/gkz446.

STAR★METHODS

KEY RESOURCES TABLE

REAGENT or RESOURCE	SOURCE	IDENTIFIER
Antibodies		
NFκB-p65	Cell Signaling Technology	Cat# 8242; RRID: AB_10859369
pS536 NFκB-p65	Cell Signaling Technology	Cat# 3033; RRID: AB_331284
pS529 NFκB-p65	Cell Signaling Technology	Cat# 96874: RRID: AB_3099546
pS32 IκBα	Cell Signaling Technology	Cat# 2859; RRID: AB_561111
IκBα	Cell Signaling Technology	Cat# 4812; RRID: AB_10694416
NFκB-p105/p50	Cell Signaling Technology	Cat# 13586; RRID: AB_2665516
GAPDH	Santa Cruz Biotechnology	Cat# sc-365062; RRID: AB_10847862
YAP xp	Cell Signaling Technology	Cat# 14074; RRID: AB_2650491
YAP (63.7)	Santa Cruz Biotechnology	Cat# sc-101199; RRID: AB_1131430
active YAP	Abcam	Cat# ab205270; RRID: AB_2813833
pLATS-HM	Cell Signaling Technology	Cat# 8654; RRID: AB_10971635
LATS1	Cell Signaling Technology	Cat# 3477; RRID: AB_2133513
LATS2	Cell Signaling Technology	Cat# 5888; RRID: AB_10835233
p-YAP(S127)	Cell Signaling Technology	Cat# 13008; RRID: AB_2650553
pS176/180 IKK	Cell Signaling Technology	Cat# 2697; RRID: AB_2079382
pS63 cJun	Cell Signaling Technology	Cat# 91952; RRID: AB_2893112
cJun	Cell Signaling Technology	Cat# 9165; RRID: AB_2130165
p-PKC substrates	Cell Signaling Technology	Cat# 6967; RRID: AB_10949977
p-PKA substrates	Cell Signaling Technology	Cat# 9624; RRID: AB_331817
p-AKT substrates	Cell Signaling Technology	Cat# 9614; RRID: AB_331810
p-AMPK substrates	Cell Signaling Technology	Cat# 5759; RRID: AB_10949320
p-CDK substrates	Cell Signaling Technology	Cat# 9477; RRID: AB_2714143
p-ATM/ATR substrates	Cell Signaling Technology	Cat# 6966; RRID: AB_10949894
pT202/Y204 ERK1/2	Cell Signaling Technology	Cat# 4370; RRID: AB_2315112
ERK1/2	Cell Signaling Technology	Cat# 9107; RRID: AB_10695739
pT180/Y182 p38	Cell Signaling Technology	Cat# 4511; RRID: AB_2139682
p38	Cell Signaling Technology	Cat# 8690; RRID: AB_10999090
S6	Cell Signaling Technology	Cat# 2217; RRID: AB_331355
pS235/236 S6	Cell Signaling Technology	Cat# 2211; RRID: AB_331679
p70 S6K	Cell Signaling Technology	Cat# 9202; RRID:AB_331676
pT389 p70 S6K	Cell Signaling Technology	Cat# 9205; RRID: AB_330944
PARP	Cell Signaling Technology	Cat# 9542; RRID: AB_2160739
Caspase 3	Cell Signaling Technology	Cat# 14220; RRID: AB_2798429
Cleaved Caspase3	Cell Signaling Technology	Cat# 9664; RRID: AB_2070042
Caspase 8	Cell Signaling Technology	Cat# 4790; RRID: AB_10545768
MLKL	Cell Signaling Technology	Cat# 14993; RRID: AB_2721822
RIP	Cell Signaling Technology	Cat# 3493; RRID: AB_2305314
pS166 RIP	Cell Signaling Technology	Cat# 65746; RRID: AB_2799693
LC3B	Sigma	Cat# L7543; RRID: AB_796155

(*Continued on next page*)

Continued

REAGENT or RESOURCE	SOURCE	IDENTIFIER
Chemicals, peptides, and recombinant proteins		
Dulbecco's Modified Eagle Medium	Sigma-Aldrich	Cat# D5796
Fetal Bovine Serum	HyClone	Cat# SH30071.03
0.05% trypsin -EDTA solution	Thermo Fisher Scientific	Cat# R001100
Agarose, low gelling temperature	Sigma-Aldrich	Cat# A9045-50G
PerfeCta SYBR Green SuperMix	Quanta	Cat# 95054-500
THUNDERBIRD® SYBR® qPCR Master Mix	Diagnocine.com	Cat# YB-QPS-201-5PK
PolyJet *In Vitro* DNA Transfection Reagent	SignaGen	Cat# SL100688
TRIzol™ Reagent	Thermo Fisher Scientific	Cat# 15596026
Critical commercial assays		
RNeasy Kits	QIAGEN	Cat# 74106
qScript cDNA synthesis kit	Quantabio	Cat# 95047-100
iScript™ cDNA Synthesis Kit	Bio-Red	Cat# 1708891
Lipofectamine™ RNAiMAX Transfection Reagent	Thermo Fisher Scientific	Cat# 13778075
Lipofectamine™ 3000 Transfection Reagent	Thermo Fisher Scientific	Cat# 3000015
Fibronectin (human)	AdvancedBiomatrix	Cat# 5080
Sulfo-SANPAH (sulfosuccinimidyl 6-(4′-azido-2′-nitrophenylamino)hexanoate)	Thermo Fisher Scientific	Cat# 22589
Experimental models: Cell lines		
C28I2	Sigma-Aldrich	Cat# SCC043
Oligonucleotides		
Primer: ADAMTS4 Forward: 5′-GAGGAGGAGATCGTGTTTCCA-3′	This paper	N/A
Primer: ADAMTS4 Reverse: 5′-CCAGCTCTAGTAGCAGCGTC-3′	This paper	N/A
Primer: IL1β Forward: 5′- AAACAGATGAAGTGCTCCTTCCAGG -3′	This paper	N/A
Primer: IL1β Reverse: 5′- TGGAGAACACCACTTGITGCTCCA -3′	This paper	N/A
Primer: ANKRD1 Forward: 5′- AGTAGAGGAACTGGTCACTGG -3′	This paper	N/A
Primer: ANKRD1 Reverse: 5′- TGTTTCTCGCTTTTCCACTGTT -3′	This paper	N/A
Primer: AMOTL2 Forward: 5′- GCTCGTTGAGTGAACGGCT -3′	This paper	N/A
Primer: AMOTL2 Reverse: 5′- CATGAGCTAGTACAACATGAGGG -3′	This paper	N/A
Primer: CTGF Forward: 5′- ACCGACTGGAAGACACGTTTG -3′	This paper	N/A
Primer: CTGF Reverse: 5′- CCAGGTCAGCTTCGCAAGG -3′	This paper	N/A
Primer: CYR61 Forward: 5′- CTCGCCTTAGTCGTCACCC -3′	This paper	N/A
Primer: CYR61 Reverse: 5′- CGCCGAAGTTGCATTCCAG-3′	This paper	N/A
Primer: GAPDH Forward: 5′- GGAGCGAGATCCCTCCAAAAT -3′	This paper	N/A
Primer: GAPDH Reverse: 5′- GGCTGTTGTCATACTTCTCATCG -3′	This paper	N/A
Primer: 18S rRNA Forward: 5′-GTAACCCGTTGAACCCCATT-3′	This paper	N/A
Primer: 18S rRNA Reverse: 5′-CCATCCAATCGGTAGTAGCG-3′	This paper	N/A
Primer: MMP1 Forward: 5′- AAAATTACACGCCAGATTTGCC-3′	This paper	N/A
Primer: MMP1 Reverse: 5′- GGTGTGACATTACTCCAGAGTTG-3′	This paper	N/A
Primer: MMP9 Forward: 5′- TGTACCGCTATGGTTACACTCG -3′	This paper	N/A
Primer: MMP9 Reverse: 5′- GGCAGGGACAGTTGCTTCT-3′	This paper	N/A
Primer: MMP13 Forward: 5′-ACTGAGAGGCTCCGAGAAATG-3′	This paper	N/A
Primer: MMP13 Reverse: 5′- GAACCCCGCATCTTGGCTT-3′	This paper	N/A
Primer: COL2A1 Forward: 5′- TGGACGATCAGGCGAAACC-3′	This paper	N/A
Primer: COL2A1 Reverse: 5′- GCTGCGGATGCTCTCAATCT -3′	This paper	N/A

(*Continued on next page*)

Continued

REAGENT or RESOURCE	SOURCE	IDENTIFIER
Primer: PTGS2 Forward: 5′- TAAGTGCGATTGTACCCGGAC-3′	This paper	N/A
Primer: PTGS2 Reverse: 5′- TTTGTAGCCATAGTCAGCATTGT -3′	This paper	N/A
Primer: NOS2 Forward: 5′- TTCAGTATCACAACCTCAGCAAG -3′	This paper	N/A
Primer: NOS2 Reverse: 5′- TGGACCTGCAAGTTAAAATCCC -3′	This paper	N/A
siPKC ζ#1: hs.Ri.PRKCZ.13.1-SEQ1: rGrUrGrCrArUrGrArUrGrArCrGrArGrGrArUrArUrUrGrACT	IDT-DNA	N/A
siPKCζ#1:hs.Ri.PRKCZ.13.1-SEQ2: rArGrUrCrArArUrArUrCrCrUrCrGrUrCrArUrCrArUrGrCrArCrCrA	IDT-DNA	N/A
siPKC ζ#2: hs.Ri.PRKCZ.13.2-SEQ1: rArGrArArUrGrArCrCrArArArUrUrUrArCrGrCrCrArUrGAA	IDT-DNA	N/A
siPKC ζ#2: hs.Ri.PRKCZ.13.2-SEQ2: rUrUrCrArUrGrGrCrGrUrArArArUrUrUrGrGrUrCrArUrUrCrUrUrC	IDT-DNA	N/A
Recombinant DNA		
PsPAX2	Addgene	Cat# 12260
pMD2.G	Addgene	Cat# 12259
LentiCRISPR-v2-sgYAP	This paper	N/A
LentiCRISPR-v2- sgLATS1	This paper	N/A
pLentiGuide-Hygro-sgLATS2	This paper	N/A
pcDNA-MST2-3xFlag	This paper	N/A
pcDNA3.1-LATS1-HA	This paper	N/A
pcDNA3.1 (+)	Invitrogen	Cat# V790-20
pCMV-p65- NFκB-p65	This paper	N/A
Software and algorithms		
ImageJ 1.53k Java 13.0.6	National Institutes of Health	https://imagej.nih.gov/ij
GraphPad Prism version 10.1.1	GraphPad	https://www.r-project.org/
R version 4.3.1	R Core Team	https://www.graphpad.com/

RESOURCE AVAILABILITY

Lead contact

Further information and requests for data, resources, and reagents should be directed to and will be fulfilled by the lead contact, Zhipeng Meng (zxm282@med.miami.edu).

Materials availability

All reagents generated in this study are available from the lead contact without restriction.

Data and code availability

- Original data related to this paper are available upon request and will be shared by the lead contact. RNA-Seq data were downloaded from a publicly archived GEO database. The accession number is GSE179716. Original western blot images are presented in Data S1.
- This paper does not report the original code.
- Any additional information required to reanalyze the data reported in this paper is available from the lead contact upon request.

EXPERIMENTAL MODEL AND STUDY PARTICIPANT DETAILS

Preparation of 3-dimensional chondrocyte-agarose constructs

The C28/I2 human chondrocytes were cultured in T-75 flasks with Dulbecco's Modified Eagle Medium supplemented with 10% (v/v) fetal bovine serum, and 1% (v/v) antibiotic in an incubator at 37°C and 5% CO_2. Once cells reached ~90-95% confluency, they were detached from the flasks using 0.05% trypsin -EDTA solution, centrifuged, and resuspended in DMEM to create a cell solution of 2 x 10^7 cells/mL. 4% ultra-low gelling temperature agarose was dissolved in 1x D-PBS and autoclaved at 120°C for 15 min followed by maintaining at 37°C. The cell solution and 4% agarose were mixed at a 1:1 ratio to encapsulate 1 x 10^6 cells in 2% agarose. The cell-agarose suspension was

pipetted to a three-dimensional (3D) cylindrical constructs ("discs") (8 mm in diameter, 2 mm in thickness), and cooled for agarose solidification.[75]

2D static compression

A stainless-steel cylinder weight (12 mm diameter) of 8.9 g was placed on the top of an agarose disk in contact with chondrocytes cultured on 12 mm Trans-wells with 0.4 μm pore (Figure 1A).[27] A condition of compressive stress of 5.79 mmHg for 16 h was applied to the chondrocytes, which can result in >30% high strain based on the mechanical properties of chondrocytes from 2D culture.[28] In a control group, only the agarose disk was placed on chondrocytes.

3D static compression

The 3D chondrocyte-agarose constructs were each cultured in 2 mL of DMEM supplemented with 10% FBS and 1% antibiotic for 24 hours prior to compressive loading experiments. Samples subjected to compressive loading were placed in a custom-designed bioreactor (Figure S1). To ensure an equal static compressive strain, a displacement-control approach was used for all testing.[43]

Strains of 20% were implemented in the dose-response experiment to develop a relationship between strain magnitude and cell mechano-response. At the 20% strain level, we observed increased inflammatory and catabolic gene expression in chondrocytes. Thus, 20% strain for 4 hours was used for the compressive loading experiments to evaluate the Hippo pathway. Furthermore, to perform the compression evaluations the samples were placed in separate custom-made chambers with 600 μL of DMEM. All experiments were conducted in the tissue incubator at 37°C and 5% CO_2 for 4 hours. Uncompressed samples were used as control groups.

METHOD DETAILS

Quantitative real-time PCR

Immediately following compression, cell-agarose constructs were collected and homogenized in 1 mL of TRIzol™ Reagent. NA was extracted using RNeasy Kits from QIAGEN, as described previously.[76] cDNA was synthesized using cDNA Synthesis Kit, following the manufacturer's instructions. qRT-PCR was carried out using SYBR Green SuperMix with Quant studio 3. The expression of GAPDH or 18S rRNA was used as an endogenous control. Gene expression levels were quantified using the $2^{-\Delta\Delta Ct}$ method and normalized to expression levels of the respective control group.[77]

CRISPR/Cas9 gene deletion in chondrocytes

To delete the LATS1 and LATS2 genes in C28/I2 chondrocytes, we employed lentiviral vectors carrying Cas9 and specific guide RNAs (gRNAs) targeting these genes. The LentiCRISPRv2 plasmid, containing a gRNA for LATS1, and the pLenti-Guide-hydro plasmid, harboring a gRNA for LATS2, were used to generate the respective lentiviruses. These lentiviruses were then utilized to transduce C28/I2 cells.

The lentiviral packaging was achieved by co-transfecting the LentiCRISPRv2 or pLenti-Guide-hydro plasmids with the packaging plasmids PsPAX2 and pMD2.G into HEK293T cells using the PolyJet *In Vitro* DNA Transfection Reagent. Following transfection, the lentiviruses were harvested and used to infect C28/I2 cells for 48 hours.

To select cells with successful gene knockouts, we applied a selection pressure using 2 μg/ml puromycin and 200 μg/ml hygromycin for 3-5 days. Subsequently, the cells were maintained in media containing a reduced concentration of puromycin or hygromycin.

The efficiency of LATS1 and LATS2 gene deletions was verified through western blot analysis using specific antibodies against LATS1 and LATS2. We also employed CRISPR/Cas9 to delete the YAP gene in C28/I2 cells using the same procedure. The guide RNA sequences targeting LATS1/2 were described previously.[23] guide RNA sequences targeting YAP as follows:

#GATGAACCTTTACCAAAACG.

RNA interference in chondrocytes

Duplex siRNA-mediated PKCζ gene knockdown was performed with Lipofectamine™ RNAiMAX Transfection Reagent, following the manufacturer's instructions. Briefly, 2 x 10^5 C28/I2 cells were plated in a 6-well plate and transfected with 30 nM siRNA using 9 μL/well of Lipofectamine RNAiMAX. Cells were harvested 2 days after siRNA transfection.

Plasmids co-transfection in chondrocytes

Total 2.5 μg pcDNA3.1-MST2-3xFlag, pcDNA3.1-LATS1-HA, pCMV-p65- NFκB-p65 plasmids were transfected to siPKCζ knockdown chondrocyte using Lipofectamine™ 3000 Transfection Reagent following the manufacturer's instructions.

Western blot analysis

Either cell-agarose constructs or chondrocytes (monolayer culture) were lysed with 1 x SDS PAGE Sample buffer after 4-hour mechanical loading. 10 μL protein samples were loaded and separated on 9% or 4%-20% SDS PAGE gels or 7.5% Phostag gels, and then were transferred to PVDF membranes and blotted with the antibodies previously described.[53]

The quantification of the regular and Phostag immunoblots was carried out using ImageJ software. In the case of Phostag analysis, we calculated a weighted-average mean value for each lane. Specifically, the 7.5% Phostag SDS-PAGE yielded five distinct bands for YAP proteins, ranging from 70 kDa (non-phosphorylated) to 100 kDa (fully phosphorylated). The weights assigned to these five bands were 0%, 25%, 50%, 75%, and 100%, respectively, in ascending order from 70 kDa to 100 kDa. To determine the total phosphorylation, we multiplied the grayscale values of each band by its corresponding weight. The final phosphorylation level of YAP was then calculated by dividing the sum of the weighted grayscale values of the phosphorylated bands by the total grayscale values of all five bands.

Polyacrylamide hydrogel substrate

We prepared polyacrylamide gels with varying moduli of elasticity to mimic different levels of extracellular matrix (ECM) stiffness, using different proportions of acrylamide and bis-acrylamide. The protocol followed the method previously reported.[78] After coating with 10 μg/ml fibronectin (human) at 37°C overnight, 8×10^4 cells were seeded onto the gels. Proteins and RNA were harvested after 24 hours.

Bioinformatic analysis

Raw count data of Database: GSE179716 was downloaded from the GEO database. Differential gene expression analysis was performed using DESeq2[79] with the criteria of log2FoldChange>0 and p-value < 0.05 to identify genes that were differentially expressed. Then Gene Set Enrichment Analysis (GSEA) was performed using the 'c5.go.v2023.1.Hs.symbols.gmt' gene set obtained from the MSigDB database.[80]

In the GSE179716 dataset, cartilage samples were classified based on the Outerbridge score for macroscopic appearance and the OARSI score for histological evaluation. These samples were obtained from patients undergoing total knee joint arthroplasty, allowing the researchers to distinguish between early-stage (preserved) and late-stage (damaged) OA. The Outerbridge score ranges from 0 (normal) to 4 (severely damaged), while the OARSI score ranges from 0 to 24, with higher scores indicating more severe damage. Samples were considered preserved if they had an Outerbridge score of 1 or less and an OARSI score of less than 12. Samples with higher scores were considered damaged.

To identify the top 200 transcription factors (TFs) responsible for the observed changes in gene expression using ChEA3,[81] we performed Kinase Enrichment Analysis 3 (KEA3)[58] to predict the upstream kinases that play a role in the mechanoresponses of chondrocytes.

QUANTIFICATION AND STATISTICAL ANALYSIS

Statistical analysis

GraphPad Prism 10 software was used for all statistical analyses. The data are presented as mean ± SEM. For comparisons between any two groups, statistical significance was assessed using a two-tailed unpaired Student's t-test. In figures where multiple groups are displayed, statistical significance was evaluated individually for each possible pair using Student's t-tests, rather than applying one-way ANOVA, to ensure biological relevance in the comparisons made. Only in cases where a global assessment of variance was biologically justified did we employ one-way ANOVA, which was followed by Tukey's multiple comparisons test if applicable. Statistical significance is indicated within each graph, with a p-value of less than 0.05 being considered significant.